H.O. Stekler Research Program on Forecasting

WORKING PAPER SERIES

Modelling the dependence between recent changes in polar ice sheets: Implications for global sea-level projections

Luke P. Jackson

Katarina Juselius

Andrew B. Martinez

Felix Pretis

Working Paper No. 2025-002

April, 2025

H. O. STEKLER RESEARCH PROGRAM ON FORECASTING
Department of Economics
Columbian College of Arts & Sciences
The George Washington University
Washington, DC 20052
https://cer.columbian.gwu.edu/ho-stekler-research-program-forecasting

Modelling the dependence between recent changes in polar ice sheets: Implications for global sea-level projections

Luke P. Jackson*, Katarina Juselius†, Andrew B. Martinez‡, Felix Pretis§

April 2, 2025

Abstract

Changes to the mass of the polar ice sheets are of scientific and socio-economic importance due to their effect on the wider Earth system and the potential to dominate future sea-level rise. Uncertainty remains around the joint behaviour of these ice sheets, leading sea-level modellers to make assumptions about their interdependence when making projections. We use a multi-cointegration vector autoregression model to assess the statistical relationships between time series of Greenland, West, and East Antarctic ice mass change (1992-2010). Since the ice sheet response to climate forcing integrates over time, we explore three alternative model specifications. We compare I(2) models of cumulative changes in ice mass (levels) with an I(1) model of changes in ice mass (rates), explore their model dynamics, and evaluate the out-of-sample forecasts (2011-2023) against observations. Our results support the use of an I(2) model, which identifies a significant relationship between Greenland and West Antarctica, and a persistent trend in both ice sheets that is correlated with global ocean heat content. Extensions of these forecasts to 2100 show Greenland and Antarctica contributions to global sea level that agree with projections from physical-process models and structured expert judgment compatible with high-emission scenarios.

Keywords: Cointegration; dynamic analysis; ice sheets; sea level

JEL classifications: Q54, C32, C51, C52, C53

*Department of Geography, Durham University; Climate Econometrics at Nuffield College, University of Oxford. Contact: luke.p.jackson@durham.ac.uk.

†Department of Economics, University of Copenhagen. Contact: Katarina.Juselius@econ.ku.dk.

‡Office of Macroeconomic Analysis, U.S. Department of the Treasury; H. O. Stekler Research Program on Forecasting, The George Washington University; School of Advanced International Studies, Johns Hopkins University; Climate Econometrics at Nuffield College, University of Oxford. Contact: Andrew.Martinez@treasury.gov.

§Department of Economics, University of Victoria; Climate Econometrics at Nuffield College, University of Oxford. Contact: fpretis@uvic.ca.

1 Introduction

Understanding and accurately modelling changes in the mass of the polar ice sheets is of crucial scientific and socio-economic importance due to their effect on the wider Earth system (Fox-Kemper et al., 2021). One direct impact of recent ice sheet mass loss is an increasing contribution to global mean sea-level rise (20% in 1993 to 34% in 2013; Chen et al. 2017, Mouginot et al. 2019, Rignot et al. 2019). Estimates of global coastal damages from sea-level rise in 2100 vary from US$ 1.4 trillion per year (0.25% of global GDP) to US$ 14 trillion per year (2.8% of global GDP) under stringent and high emissions scenarios respectively (without adaptation; Jevrejeva et al. 2018). The future contribution to sea-level rise from the polar ice sheets is a key source of this 10-fold increase.

Projections of future sea-level rise often rely on characterizing the relationship between individual sea-level components (including ice sheets) so that these can be correctly implemented within a modelling framework (e.g., Oppenheimer et al., 2016, Bamber et al., 2019, Kopp et al., 2014, Fox-Kemper et al., 2021). Given the high likelihood that the end-of-century contributions to global sea-level change will be dominated by the Greenland and Antarctic ice sheets (e.g., Fox-Kemper et al., 2021), it is therefore important to improve the characterization of these relationships.

Observations of the changes in ice sheet mass have grown in number and accuracy drawing upon numerous remote and in-situ methods (e.g., Barletta et al. 2013, King et al. 2018, Mouginot et al. 2019, Rignot et al. 2019) leading to composite reconstructions as well (e.g., Shepherd et al. 2012, 2018, 2019). However, there remains the ongoing challenge of modelling ice sheets given their size, complex physical behaviour, range of self-governing and climate feedbacks, potential nonlinearities, and variable time-scale response. These issues, as well as the high computational demands implied therein mean that both contiguous ice sheets (Greenland and Antarctica) are rarely modelled jointly (e.g. Vizcaíno et al. 2010) or within a wider Earth System modelling framework (e.g., Smith et al., 2021). Therefore, the degree to which their individual responses co-move due to climate adjustments (e.g., atmosphere and ocean forcing) remains an outstanding question – especially at the seasonal to decadal timescales measured by observation. From the perspective of a sea-level modeller, this uncertainty poses a challenge when constructing probabilistic projections as the covariance between individually modelled sea-level components can influence low-probability high-end future sea levels (e.g., Le Bars, 2018). Fox-Kemper et al. (2021) addressed this challenge with the use of statistical ice sheet emulators trained on behaviour from physical process ice sheet models with global temperature as the conditional parameter; see also Grinsted et al. (2022).

In this paper we examine the statistical properties of, and co-movement between the Greenland, West and East Antarctic ice sheets, which appear to show non-stationary changes over the last 30 years. By estimating multi-cointegration models we test for non-stationarity as well as feedback and potential unstable behaviour, consistent with being near or having crossed a tipping point. Our results help refine models of inter-dependence of the ice sheets motivated by physical relationships. We then apply these models to construct out-of-sample forecasts (sea-level projections) to 2100 and compare them to recent physical process-driven and expert-based projections.

This approach allows us to explore the dynamics and interactions between the polar ice sheets using physically motivated statistical models while simultaneously embedding and testing for the relevance of currently hypothesised drivers. Second, multi-cointegration is both valid and informative for non-stationary time series, unlike simple linear relationships that have previously been applied in this context (e.g., Bamber and Aspinall, 2013, Le Bars, 2018). Crucially, the model allows us to test for and quantify feedback between ice sheets and to model potentially explosive behaviour, which can be indicative of being near or having crossed a tipping point. Finally, our framework enables us to explore whether the series should be modelled as the total mass anomaly (i.e. in levels) using a complex model, or as mass balance (i.e. in differences) using a simpler model, and if there is a cost of choosing one approach or another.

We find that the joint system of polar ice sheet mass anomalies is well-approximated by $I(2)$ processes with two multi-cointegrating vectors. The two long-run equilibrium relationships can be interpreted as a positive relationship between Greenland and West Antarctica and an intra-antarctic relationship between West and East Antarctica. We show that these long-run relationships are not captured by simple correlations and that information is lost by treating one or all of the ice sheets as $I(1)$ processes and modelling them in differences. The dynamics of the model indicate that the estimated stochastic trends closely follow the evolution of ocean heat content and CO_2 concentrations and there is evidence of instabilities within the system, especially for Greenland, which exhibits explosive behaviour suggesting accelerating ice loss. The out-of-sample forecast performance supports our in-sample estimates, although there is evidence that choosing a simpler, more flexible model can improve forecasts in the short-to-medium term. Our results also provide empirical evidence of the behaviour of the Greenland ice sheet being consistent with being near to a tipping point and undergoing a tipping phase (Boers and Rypdal, 2021). Over the longer-term, the forecasts from our model to 2100 align with the upper end of recent physical process-driven and expert-based global mean sea-level projections, highlighting the importance of correctly characterising these relationships.

The paper proceeds as follows. The next section outlines the mechanisms and drivers of ice sheet mass change, since it is these observations that we seek to understand. We also summarise attempts to simulate this behaviour using simple-physical, or physically-motivated ice sheet models. Section 3 describes the ice sheet mass data used in our analysis and shows why applying simple linear models between the ice sheet regions is misleading. Section 4 describes the general, unrestricted multi-cointegration model and section 5 discusses how we test for and impose restrictions upon it. Section 6 considers three alternative model specifications based on an ice sheet-Earth system understanding. Section 7 analyses the model by examining drivers of the stochastic trend (7.1), explores the model dynamics (7.2), and compares the out-of-sample forecasts to the recent physical science literature (7.3 and 7.4). Section 8 concludes.

2 Mechanisms and drivers of ice sheet mass change

Changes in the total ice sheet mass can be separated into surface mass balance and ice sheet dynamics. Surface mass balance (SMB) is primarily caused by the net change in precipitation (via snowfall), runoff, and surface melt. On the other hand, ice sheet dynamics relate to internal ice sheet processes and interactions with ocean and land interfaces.

The Greenland ice sheet (GrIS) has experienced rapid warming over the last 30 years with higher winter ($\sim$5°C) and summer ($\sim$2°C) surface-air temperatures (Hanna et al., 2021). This warming causes more surface melting but also greater snowfall due to increased moisture retention within the air. Numerous factors contribute to this warming beyond the global average including enhanced solar radiation, melt-albedo and melt-elevation feedbacks (e.g. Lim et al. 2016, Hofer et al. 2017) as well as atmospheric blocking from global teleconnections (e.g. Li et al. 2021, Hanna et al. 2024). The net result is a negative SMB (where surface melt outpaces snowfall) that has continued to increase since 2000. In addition, marine-terminating glaciers have increased mass loss from ice sheet dynamics, which is partly caused by ice-ocean interactions due to ocean circulation and warming (e.g. Khan et al. 2014, King et al. 2018). At present, SMB and ice sheet dynamics contribute 67% and 33% to total mass loss respectively (Mouginot et al. 2019) though this ratio is not constant through time.

The Antarctic ice sheet (AIS) can be separated into three distinct regions: West (WAIS) and East (EAIS) Antarctica separated by the Trans-antarctic Mountains, and the Antarctic Peninsula (APIS). The WAIS mainly lies upon bedrock that is below sea level and deepens inland making it susceptible to unstable, accelerating mass loss as the submarine surface area increases following melting at it's front (e.g. Joughin and Alley 2011, Bamber et al. 2018). The EAIS mainly lies on bedrock above sea level and is considered more stable than WAIS (despite

a few marine-based sectors remaining susceptible to ocean melting). Average temperatures in Antarctica have remained stable over the last 30 years however regional trends over shorter multi-annual timescales reveal more complex fluctuations due to ice-albedo feedback, and a range of atmospheric drivers including global teleconnections, especially over APIS and the South Pole (see Rignot et al. 2004, Post et al. 2019, Clem et al. 2020, Li et al. 2021, Hanna et al. 2024).

Cumulative anomalies of SMB across all three regions are dominated by inter-annual variability with no clear trend over the past 40 years (Rignot et al., 2019). However, observations for the last decade indicate that this may be becoming negative for both WAIS and EAIS (Otosaka et al., 2023). Ice dynamics (via discharge) is the primary contributor to mass loss across these regions. The dynamics of ice streams and ice shelves at the edges of the AIS control the interior ice sheet flow outward. The coastal ice margins are susceptible to ocean forcing such as the warm, deep water component of the Antarctic circumpolar current (Pattyn et al., 2018). Although smaller scale factors have regional effects, at a continental scale such oceanic changes are reflected through factors such as increased ocean heat content (e.g., Dinniman et al., 2012). SMB and dynamic processes contribute around 20% and 80%, 30% and 70%, and -10% and 110% to total mass loss for WAIS, EAIS and APIS respectively (Rignot et al., 2019).

The use of complex, physically-based ice sheet models is essential to reconstruct and project regional changes in ice sheet behaviour. At present, the large-scale (e.g., WAIS or GrIS) changes in SMB are well modelled (e.g. Church et al., 2013, Pattyn et al., 2018, Oppenheimer et al., 2019, Fox-Kemper et al., 2021). However, for ice dynamics there remain differing perspectives on the physical mechanisms at work and their sensitivity to climate forcing (e.g. DeConto and Pollard, 2016, Edwards et al., 2019, Golledge et al., 2019, DeConto et al., 2021, Seroussi et al., 2024). Such differences led Fox-Kemper et al. (2021) to construct two different global sea-level projections for the same climate scenario (medium and low confidence) that reflected this "deep uncertainty" as well as covariance between ice sheet components driven solely by temperature, rather than based on observation. An important alternative method used to evaluate both deep uncertainty and covariance between ice sheet components is structured expert judgement (e.g., Bamber and Aspinall, 2013, Bamber et al., 2019), though such approaches lack dynamic covariance and observational verification - an aspect that can be addressed through econometric modelling.

Cointegration analysis allows for dynamic correlations in a non-stationary setting by explicitly allowing for feedback while also allowing for being near or having crossed a tipping point through possibly explosive behaviour. It was originally formulated in a bivariate setting by

Engle and Granger (1987), with extensions to multi-cointegration by Granger and Lee (1989), as an empirical approach for understanding the dynamics of co-movements between two or more data series in a non-stationary setting over time. Johansen (1988) and Johansen and Juselius (1990) generalized cointegration analysis for $I(1)$ systems while Johansen (1997, 2006) did so for $I(2)$ systems.

These methods have a long history in time series econometrics and are also increasingly used to analyse dynamic interactions between series in climatological data; for example see Schmith et al. (2012), Kaufmann and Juselius (2013), Pretis (2020) and Bruns et al. (2020) among others. Our analysis is also comparable in nature to Diebold and Rudebusch (2021), Coulombe and Göbel (2021) and Diebold et al. (2023) who estimate time-series models of arctic sea ice extent. Similar to those approaches, we estimate empirical models of climate processes and generate true out-of-sample forecasts (rather than projections on a specific temperature pathway). However, unlike Diebold and Rudebusch (2021) who focus on single-equation models of sea ice extent, we model the joint system of polar ice sheets and explore the performance of $I(1)$ relative to $I(2)$ multi-cointegration models.

3 Ice Sheet Measurements and Simple Correlations

We analyse the Greenland and Antarctic ice sheets using the Ice Sheet Mass Balance Exercise (IMBIE) from Shepherd et al. (2012). Monthly, total ice mass balances (*Gt per month*) are available from 1992-2012 for GrIS, WAIS and EAIS (Figure 1, Column 2). APIS is combined with WAIS given their geographical proximity and the relatively small size of APIS. Mass balances are constructions from an ensemble of methods: satellite altimetry, interferometry, and gravimetry that are post-processed using common regions, time intervals, SMB models (where applicable) and glacial isostatic adjustment corrections (Shepherd et al. 2012).

While IMBIE has been extended multiple times through 2020, see Shepherd et al. (2018, 2019, 2021) and Otosaka et al. (2023), the updated data were processed using annual average growth rates such that their usefulness in being able to model the monthly time series is limited. As a result, our analysis focuses on the original data until 2012 and uses the updated data only to evaluate the out-of-sample forecasts. Future research could consider alternative data sources such as those from Wiese et al. (2022) and Sasgen et al. (2019) which are available since 2003 but exhibit more noise and have a large number of missing observations.

The data are available as total ice mass balance (*Gt per month*) and the ice mass anomaly (Gt) relative to 1992 is integrated from the mass balance (Figure 1, Column 3). We also

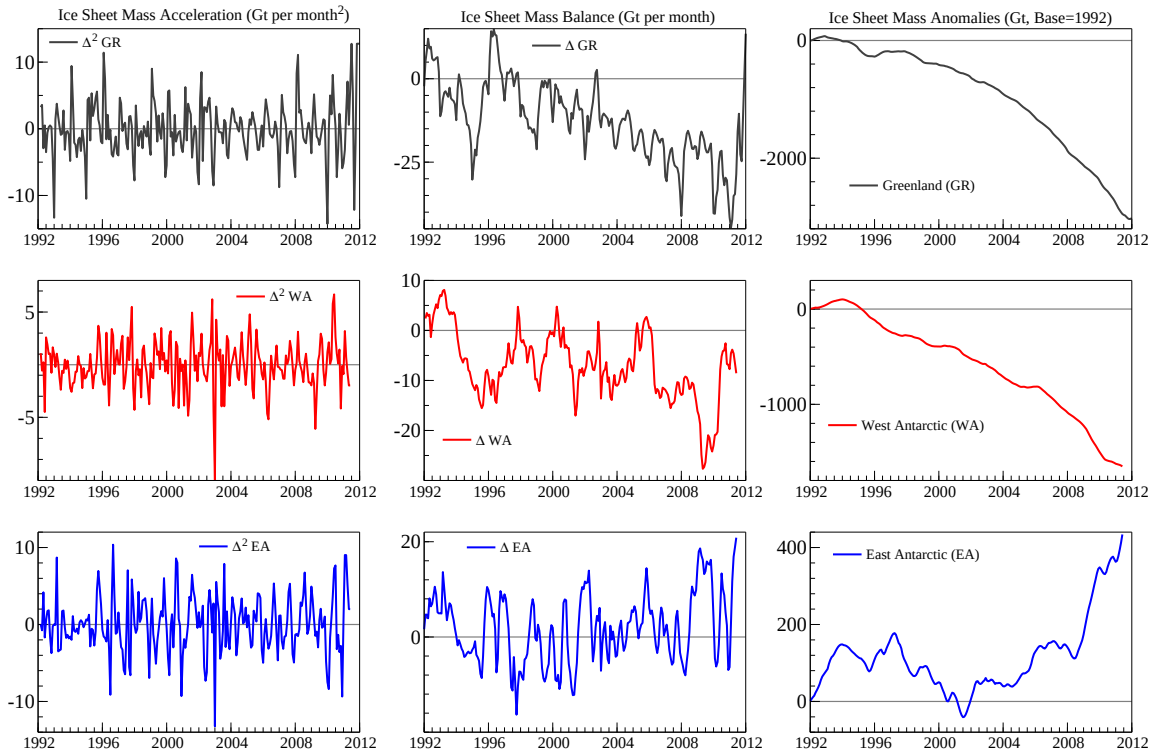

Note: Gt stands for Gigatonnes.

Figure 1: Ice Sheet Acceleration, Mass Balance, and Mass Anomalies 1992-2012. Mass balance data from Shepherd et al. (2012)

differentiate total ice mass balance to produce total ice mass acceleration[1] (*Gt per month*^{2}) (Figure 1, Column 1). While there are no clear trends or cycles in the accelerations, GrIS and WAIS both exhibit strong negative trends in their mass balance and EAIS exhibits a weaker positive trend. There is also clear seasonality in all three mass balances, a feature primarily due to the annual cycle of SMB (e.g., Mouginot et al., 2019, Rignot et al., 2019) but also ice dynamics in Greenland (King et al., 2018). The total ice mass anomaly shows explosive behaviour over time, reflecting the underlying trend in ice mass balance, though this behaviour is not synchronous beginning in 2001 for EAIS. Lastly, there are several obvious outliers (2003: EAIS, WAIS; 2012: GrIS) within the mass accelerations indicating either a major short-term ice mass event (Antarctica: likely anomalous snowfall; Greenland: likely high summer melt) or a change in the measurement procedure (Shepherd et al., 2012).

As mentioned earlier, attempts to jointly project the future contribution to global mean sea-level change of GrIS, WAIS and EAIS (e.g., Bamber and Aspinall, 2013, Bamber et al., 2019) applied fixed correlations between each pair using a copula-style approach to draw from each ice

[1]We use the term "ice mass acceleration" to define the first-differences in the time series of ice mass balance. We do not imply a long-term acceleration of any component in the ice sheet system (e.g., quadratic over 20 years) as such as term might be used in glaciology.

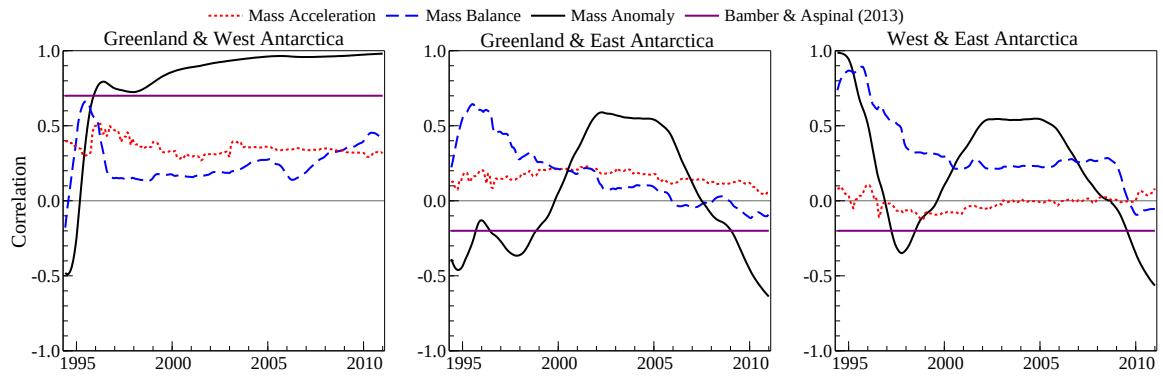

Note: Estimates start in February 1992 and are estimated using an expanding window ending initially in May 1994.

Figure 2: Recursive Estimates of Ice Sheet Correlations ending in 1994-2011

sheet's probability distribution of future change. We assess the validity of this approach using the IMBIE observations by taking recursive estimates of the bivariate correlations between the ice sheet regions for mass anomaly, mass balance and mass acceleration estimated using an expanding window over time. If the data (especially ice mass balance) were stationary then estimates of the bivariate relationships should converge as the estimation sample expands.

Figure 2 illustrates that convergence of correlations do not occur for the mass anomaly and mass balance. Although some of the correlations are the same sign as those from Bamber and Aspinall (2013) their magnitude strongly relates to the series length. Furthermore, although the mass acceleration correlation is generally stable, it is also close to zero – partly because taking differences of the data removes many of the common features (e.g. annual cycle). Therefore, the use of simple correlations in sea-level projection frameworks that include non-stationary components (e.g., ice sheet mass/mass balance) is not supported by an assessment of recent observations. Conversely, while taking differences of the ice mass balance series results in information loss (e.g., the trend, annual cycle), estimates of the correlation and dependence structure between ice sheet regions are only statistically valid if the underlying series are stationary (Johansen, 2012).

We can test for stationarity using augmented Dickey and Fuller (1979) (ADF) tests for unit roots for each of the ice sheet mass anomalies and their transformations. The results in Appendix Table A.1 show that the ice sheets are all consistent with I(2) processes, although this is sensitive to the choice of lag length. Furthermore, Juselius (2014) shows that these tests are generally sensitive when the signal to noise ratio is low while Nielsen (2001) also shows that they can be distorted when the dynamics are unstable. Thus, we proceed directly to modelling the ice sheets together as a system to allow for more powerful tools.

4 Defining the Cointegrated VAR

We can jointly model the polar ice sheets using a Vector Autoregression (VAR) to account for non-stationarity, assess the validity and physical justifications for alternative order formulations, quantify feedback dynamics, and allow for being near or having crossed tipping points through explosive roots. The VAR is derived from the joint likelihood function of the full data set, $P(\mathbf{X} \mid \mathbf{X}_0;\Theta)$, where $\mathbf{X}_0$ is a matrix of initial values and $\mathbf{X}$ is a $T \times p$ data matrix of p variables, and Θ is the matrix of parameters. Assuming $P(\cdot)$ is well-represented by the normal distribution, and the lag structure can be truncated at a finite lag k without loss of information, then the mean of the conditional probabilities corresponds to the mean of the VAR. In this sense, the VAR is a convenient reformulation of the covariances of the original data.

In practice, due to extreme events and/or measurement errors, the normality assumption is often rejected when applying the VAR to data. However, extreme outliers can be controlled for by adequately designed dummy variables such that the normality assumption is satisfied. Analysis of the lag structure of the polar ice sheets using F-tests, which Nielsen (2006) shows are valid even if the data exhibits explosive behaviour, indicates that the lags can be truncated at three. The unrestricted VAR of the data in levels (i.e. the cumulative mass balance or mass balance anomaly) is therefore represented by:

$$x_t = \Pi_1 x_{t-1} + \Pi_2 x_{t-2} + \Pi_3 x_{t-3} + \mu_0 + \mu_1 t + \Psi S_t + \Phi D_t + \varepsilon_t, \quad \varepsilon_t \sim N(0, \Omega) \tag{1}$$
$$t = 1992{:}1 - 2011{:}1$$

where Ω is the residual covariance matrix; the vector $x_t = [Gr_t, WA_t, EA_t]$, where Gr_t measures the mass anomaly of the ice sheet in Greenland, WA_t in West Antarctica, EA_t in East Antarctica; μ_0 is a constant; t is a linear time trend; S_t is a vector of seasonal dummy variables and ε_t are the unexplained residuals which are designed to be white noise.

We include a vector of dummy variables $D_t = [Dp_{93:3,t}, Dp_{97:9,t}, Dtr_{03:1}Dp_{09:4,t}]$ that capture extreme observations selected as large residuals using Autometrics (Doornik, 2009) with a target size of 1%. $Dp_{xx:y}$ is 1 in 19xx:y or 20xx:y, 0 otherwise and $Dtr_{03:1}$ is 1 in 2003:1, -1 in 2003:2, otherwise 0. The impulse dummy for April 2009 may capture the Wilkins ice bridge collapse and the resulting ice shelf loss that month; see Humbert et al. (2010). The other impulses are likely measurement issues associated with individual ice sheets such as the beginning of laser altimetry measurements in March 1993, whereas the differenced impulse dummy in January 2003 captures a measurement issue across all three ice sheets due to the inclusion of new gravimetry/radar altimetry measurements; see Shepherd et al. (2012). Table 1 reports the estimates.

Table 1: Estimated dummy variable effects

	1993:3	1997:9	2003:1-2	2009:4
Gr_t	$*$	3.60 (1.40)	4.54 (2.50)	$*$
WA_t	$*$	$*$	-7.48 (-5.81)	-6.06 (-3.47)
EA_t	10.39 (4.17)	-10.30 (-4.19)	-11.94 (-6.56)	$*$
System Specification Tests				
Normality: $\chi^2(6)$			12.95[0.044]*	
Autocorrelation LM1: $\chi^2(9)$			13.69[0.134]	
Autocorrelation LM2: $\chi^2(9)$			14.72[0.099]	
ARCH LM1: $\chi^2(36)$			47.86[0.089]	
ARCH LM2: $\chi^2(72)$			114.84[0.001]**	
Univariate Specification Tests				
		ΔGr_t	ΔWA_t	ΔEA_t
Normality:		4.23 [0.121]	4.37 [0.113]	3.45 [0.178]
ARCH(2):		0.68 [0.712]	7.66* [0.022]	0.47 [0.791]

Note: t-values are in parentheses and p-values are in square brackets.

A set of mis-specification tests indicate no significant residual autocorrelation of order 1 and 2, no significant residual ARCH of order 2 - except for WA_t, but only modestly so - and no rejection of residual normality. Thus, we consider the VAR to be well-specified.

It is useful to reformulate the VAR in (1) in differences (i.e. mass balance) and levels:

$$\Delta x_t = \Pi x_{t-1} + \Gamma_1 \Delta x_{t-1} + \Gamma_2 \Delta x_{t-2} + \mu_0 + \mu_1 t + \Psi S_t + \Phi D_t + \varepsilon_t, \tag{2}$$

where $\Pi = -(I - \Pi_1 - \Pi_2 - \Pi_3)$, $\Gamma_1 = -(\Pi_2 + \Pi_3)$ and $\Gamma_2 = -\Pi_3$. The roots of the companion matrix of (2) have the necessary information about the stability of the system; see Hendry and Juselius (2001). If all the roots have modulus less than one, then x_t represents a stationary process, abbreviated $x_t \sim I(0)$. This also implies that Π is full rank. Alternatively, if all the eigenvalues are inside or on the unit circle, then x_t is a non-stationary process. Finally, if any of the roots are outside the unit circle then x_t is an explosive process. The VAR in (1) can also be reformulated in first and second order differences (i.e. mass acceleration) and levels:

$$\Delta^2 x_t = \Pi x_{t-1} + \Gamma \Delta x_{t-1} + \Gamma_{12} \Delta^2 x_{t-1} + \mu_0 + \mu_1 t + \Psi S_t + \Phi D_t + \varepsilon_t, \tag{3}$$

where $\Gamma = -(I - \Gamma_1 - \Gamma_2)$ and $\Gamma_{12} = -\Gamma_2$. Now we can further characterize the non-stationary properties of the system. If $\Pi = 0$ and Γ has full rank, then $x_t \sim I(1)$. Whereas if $\Pi = 0$ and $\Gamma = 0$, then $x_t \sim I(2)$. However, if $\Pi = \alpha\beta'$ is of reduced rank, $r < p$, but $\alpha'_\perp \Gamma \beta_\perp$ is of full rank

Table 2: The trace test statistics for the two rank indices

$p-r$	r	$s_2=3$	$s_2=2$	$s_2=1$	$s_2=0$		
3	0	107.24 [0.00]	66.43 [0.09]	50.94 [0.09]	43.90 [0.04]		
2	1		49.92 [0.04]	29.37 [0.19]	24.55 [0.07]		
1	2			13.34 [0.35]	9.97 [0.13]		
Six largest characteristic roots (modulus of)							
$r=3, s_1=0, s_2=0$		1.01	0.95	0.95	0.84	0.84	0.71
$r=2, s_1=0, s_2=1$		1.0	1.0	0.87	0.87	0.81	0.73
$r=1, s_1=1, s_2=1$		1.0	1.0	1.0	0.86	0.86	0.59
$r=0, s_1=2, s_2=1$		1.0	1.0	1.0	1.0	0.82	0.65
$r=0, s_1=1, s_2=2$		1.0	1.0	1.0	1.0	1.0	0.64

Note: p-values associated with the null hypothesis are in square brackets

where $\alpha_\perp$ and $\beta_\perp$ are orthogonal complements of α and β, then x_t is a cointegrated $I(1)$ process with β cointegrating vectors; see Johansen (1998). Alternatively, if $\Pi = \alpha\beta'$ is of reduced rank, $r < p$, and $\alpha'_\perp \Gamma \beta_\perp = \xi\eta'$ is of reduced rank $s_1 < p - r$, then x_t is a cointegrated $I(2)$ process.

The Cointegrated VAR (CVAR) represents the set of possible restrictions on the model of x_t of which the $I(0)$ model of mass anomalies is the most general and the $I(2)$ model of mass acceleration is the most constrained. It is possible to test relevant hypotheses based on scientifically valid principles because the CVAR is based on the likelihood. Hypotheses that are not rejected can be sequentially imposed, thereby narrowing down the search for the most empirically relevant and physically justifiable model among the possible set. For example, we can test whether accumulating the mass balance series into mass anomalies provides useful information or not. Assuming that it does not, then $\Pi = 0$ and including the mass anomalies provides no added benefit.

5 Determination of rank indices

The first step of the statistical analysis is to determine the division into the number of pulling and pushing forces, based on the test procedure proposed by Nielsen and Rahbek (2007) that gives the integration and cointegration indices of the model in (3).[2] Looking at Table 2, the test procedure starts with the most restricted model ($r = 0, s_1 = 0, s_2 = 3$), where r is the number of stationary multicointegrating relations, s_1 is the number of $I(1)$ trends, and s_2 the number of $I(2)$ trends.[3] The testing procedure continues to the end of the first row of Table 2, and proceeds similarly row-wise from left to right until the first non-rejection.

While the test statistics in Table 2 support at least one $I(2)$ trend in the data, they are less

[2] Pushing forces capture stochastic trends. Pulling forces capture cointegrating relations; Hoover et al. (2008).
[3] s_1 is not shown explicitly in Table 2 but is can be obtained using $s_1 = p - r - s_2$.

clear about whether there is more than one stochastic trend, or whether there are one or two cointegration relations among the ice sheets or even none. Different choices of significance level lead to different choices of rank indices. The case $(r = 0, s_1 = 1, s_2 = 2)$ is chosen based on a p-value of 0.09. However, it is nested in $(r = 0, s_1 = 3, s_2 = 0)$, which has a p-value of 0.04. The first model that has a p-value larger than 0.05 and is not nested by a model with a p-value less than 0.05 is $(r = 1, s_1 = 1, s_2 = 1)$ which is also the case that would be selected when going from the least restricted model and ending on the last model with a p-value larger than 0.05. Alternatively, the first model that has a p-value larger than 0.10 and is not nested by a model with a p-value less than 0.10 is $(r = 2, s_1 = 0, s_2 = 1)$.

We can augment the trace test results by examining the characteristic roots (i.e. eigenvalues) of the model. These are particularly valuable as they are informative of the remaining persistence in the model after a particular choice of rank indices. Table 2 reports the characteristic roots of the unrestricted CVAR, and compares them with the four candidate rank indices, going from least to most restricted, that were chosen by alternative p-values of the trace tests.

The unrestricted CVAR has one small explosive root (1.01), a complex pair of roots close to the unit circle (0.95) and a complex pair of moderately large roots (0.84). While the small explosive root is not statistically different from a unit root[4], it suggests that the ice sheets might be subject to self-reinforcing feedback dynamics. This is consistent with ice sheet theory where the mass balance is related to the mass anomaly due to an elevation feedback.[5] It also indicates the possibility of being near or having crossed a tipping point in which rapid ice mass loss occurs.[6] The unrestricted CVAR suggests that the choice of reduced rank indices should be consistent with three unit roots, provided the largest root (1.01) and the next ones (0.95) can be approximated with unit roots, or with five unit roots if, additionally, the two complex pair of roots are unit roots.

Moving down Table 2, the least restricted case chosen $(r = 2, s_1 = 0, s_2 = 1)$ is consistent with two unit roots in the data and leaves a complex pair of unrestricted moderately large roots (0.87) in the model. This reduces the total number of near unit roots with one compared to the completely unrestricted model. As we will discuss further below, the existence of two multi-cointegrated relations is consistent with a bipolar relationship between Greenland and

[4]If the explosive root were statistically significant, then it could not be restricted to a unit root, so the explosive root would remain intact in the rank restricted models.

[5]While this relates more to SMB for GrIS, it is consistent for dynamic processes like marine instability especially in WAIS.

[6]The definition of a 'tipping point' varies in the literature (see e.g. Lenton et al., 2008, Dietz et al., 2021). We consider a tipping point as explosive behaviour that does not correct to an earlier equilibrium . Ice sheet models indicate both ice sheets tip from equilibrium at about $1.5 - 2°$C above pre-industrial levels (Pattyn et al., 2018) with changes being "irreversible" on 500-year timescales. Shorter time scale fluctuations have been used to assess mass balance sensitivity in ice sheet models (Mikkelsen et al., 2018) and demonstrate non-linear mass-balance that "tips" the ice sheet into sudden mass losses that drops volume to a new "equilibrium" (>1000 years).

one or more of the Antarctic ice sheets, and an intra-antarctic relationship between East and West Antarctica. These are potential restrictions that we can impose and test for.

The next case $(r = 1, s_1 = 1, s_2 = 1)$, is consistent with three unit roots in the data and a complex pair of unrestricted large roots (0.86) in the model. $r = 1$ implies one multi-cointegrated relation between levels and differences and $s_1 = 1$ implies a single cointegrated relation among the differenced variables. Below we will impose and test the restriction that this multi-cointegrated relation is a bipolar relationship linking Greenland and Antarctica.

The most restricted case chosen $(r = 0, s_1 = 1, s_2 = 2)$ corresponds to five unit roots in the characteristic polynomial and implies that the moderately large complex pair of roots in the unrestricted model are unit roots. The largest unrestricted root is 0.64 implying that all persistent movements in the data are accounted for. The adjacent case $(r = 0, s_1 = 2, s_2 = 1)$, is consistent with three unit roots in the data and two moderately large unrestricted roots (0.82 and 0.65) in the model. Both cases imply no multi-cointegrated relations between levels and differences and are analysed by setting $\Pi = 0$ in (3) so that the CVAR collapses to an $I(1)$ analysis of Δx_t. This model therefore implies that there is no information gained from accumulating the mass balances into mass anomalies.

Overall the unrestricted model shows that there is one very persistent trend amongst the ice sheets. This appears to be approximated for reasonably well using an $I(2)$ trend in the less restricted cases. There is also persistent cyclical movement among the ice sheets as captured by the complex pair of fairly large unit roots in the three least restricted cases, with modulus around 0.89. The latter are most likely associated with persistent cyclical deviations from either the long-run or the medium-run relation. Such deviations, while quite persistent, belong nonetheless to the equilibrating forces of the model.

While the $I(2)$ models appear promising, our study is exploratory with no strong null hypothesis of what to expect. Thus, we consider each case as a potential reduction of the unrestricted CVAR. Investigating the implications of each case allows us to compare what is lost or gained in terms of understanding the mechanisms underlying the ice sheet dynamics and interactions.

6 Analysis of the Restricted CVAR Models

In this section we consider three alternative reductions of the CVAR model and their different implications for the system of ice sheets. We start by re-defining the $I(2)$ model and how to interpret the feedback and equilibrium dynamics. Then, going from the least to most restricted model, we first consider the $I(2)$ model with two multi-cointegrating relations $(r = 2, s_1 = 0, s_2 = 1)$ followed by the $I(2)$ model with one multi-cointegrating relation

$(r = 1, s_1 = 1, s_2 = 1)$. Finally, we consider the $I(1)$ model of Δx_t with two cointegrating relations $(r = 0, s_1 = 1, s_2 = 2)$.

The $I(2)$ condition is defined as a complex restriction on the $\mathbf{\Gamma}$ matrix, which means that the representation in (3) is not optimal for likelihood inference. To circumvent this, Johansen (1997) proposes the following parameterisation:

$$\begin{aligned}\Delta^2 x_t = \alpha \left[\begin{pmatrix} \beta \\ \tau_0 \end{pmatrix}' \begin{pmatrix} x_{t-1} \\ t-1 \end{pmatrix} + \begin{pmatrix} d \\ d_0 \end{pmatrix}' \begin{pmatrix} \Delta x_{t-1} \\ 1 \end{pmatrix} \right] \\ + \zeta \begin{pmatrix} \tau \\ \tau_0 \end{pmatrix}' \begin{pmatrix} \Delta x_{t-1} \\ 1 \end{pmatrix} + \Gamma_{12} \Delta^2 x_{t-1} + \Psi S_t + \Phi D_t + \varepsilon_t\end{aligned} \tag{4}$$

where α is a $3 \times r$ matrix of adjustment coefficients, β is a $3 \times r$ matrix of the long-run relationships between the ice sheets in levels, $d = -\left(\left(\alpha' \Omega^{-1} \alpha\right)^{-1} \alpha' \Omega^{-1} \Gamma\right)$ is a $3 \times r$ matrix of coefficients determined so that $(\beta' x_{t-1} + d' \Delta x_{t-1}) \sim I(0)$, $\tau = [\beta, \beta_{\perp 1}]$ is a $3 \times (r + s_1)$ matrix describing stationary relationships among the mass balances such that $\tau' \Delta x_{t-1} \sim I(0)$ where $\beta_{\perp 1}$ is the orthogonal complement of $[\beta, \beta_{\perp 2}]$, $\tau_\perp$ is the orthogonal component of τ, and ζ is a $3 \times (3 - s_2)$ matrix of medium-run adjustment coefficients. This allows us to study the feedback dynamics of both the long- and medium-run co-movements between the polar ice sheets.[7]

In (3), an unrestricted constant will cumulate twice to a quadratic trend, and a linear trend to a cubic trend. In (4), by restricting the trend to the β relations and the constant, i.e. Δt, to the d and τ relations, higher order deterministic trends can be avoided. See Doornik and Juselius (2018) and Juselius (2006, Chapter 17) for a more detailed discussion.

Juselius and Assenmacher (2017) show that four non-mutually exclusive cases describe the feedback dynamics in an $I(2)$ system. We apply their discussion to our system where for each $i \in \{Gr_t, EA_t, WA_t\}$, $j \in \{1, ..., r\}$, and $m \in \{1, 2, 3\}$:

(i) An ice sheet is equilibrium correcting in the long-run if $\alpha_{ij}\beta_{mj} < 0$ and/or $\alpha_{ij} d_{mj} < 0$;

(ii) It is equilibrium correcting in the medium-run if $d_{mj}\beta_{mj} > 0$ given $\alpha_{ij} \neq 0$;

(iii) It is equilibrium correcting to changes in deviations from the equilibrium if $\zeta'_{ij}\tau_{mj} < 0$;

(iv) For all other parameter values the ice sheet is equilibrium diverging.

However, equilibrium-diverging behaviour in one ice sheet is typically compensated by equilibrium-correcting behaviour in another reacting to the same equilibrium deviation. If these forces offset each other, then all characteristic roots are inside the unit circle and the

[7] We use CATS 3.01 in OxMetrics 8.1 to estimate the models and test for cointegration; see Doornik (2017) and Doornik and Juselius (2018).

system is ultimately stable. Thus, an ice sheet can move away from its long-run equilibrium for extended periods, but eventually it will be pushed back towards equilibrium. We consider each of the three cases not rejected by the reduced rank restrictions and analyse whether the feedback dynamics are indicative of equilibrium-correcting or equilibrium-diverging behaviour in the ice sheets.

6.1 Model 1: I(2) with 2 Multi-Cointegrating Relations ($r = 2, s_1 = 0, s_2 = 1$)

We start by considering the case with two unit roots. Table 3 reports the estimates of the multi-cointegrated relations, $\beta' x_t + d' \Delta x_t$, together with the long-run adjustment coefficients α.[8] Based on our understanding of ice sheet systems, we impose one just-identifying restriction on β_1 and two restrictions on β_2, one of which is over-identifying.[9] The restriction on β_1 implies that the first cointegrating vector specifies a long-run (positive) relationship between Greenland and West Antarctica.[10] This is consistent with the physical response of Gr and WA to common anthropogenic forcing and ocean heat content over the observed period; see Hanna et al. (2020). The restrictions on β_2 imply a long-run one-to-one (negative) relationship between East and West Antarctica. The over-identifying restriction is not rejected based on $\chi^2(1) = 1.13[0.29]$. Relaxing the over-identifying restriction between West and East Antarctica gives an implied relationship of -0.77, which is not far from our one-to-one restriction.

If we impose two over-identifying restrictions to be consistent with the correlations in Bamber and Aspinall (2013) between East and West Antarctica (-0.2) and West Antarctica and Greenland (0.7), they are strongly rejected by the data based on $\chi^2(2) = 11.47[0.003]$. Instead, we find a weaker long-run relationship between West Antarctica and Greenland than Bamber and Aspinall (2013) at about 0.41 which is significantly different from zero. We can assess the dynamics stability of the estimate by re-estimating the model recursively. The results in panel A of Appendix Figure A.1 show that it is stable.

We normalize the long-run bipolar relationship on WA_t and rewrite it as:

$$WA_t = 2.09 - 3.79t + 0.41Gr_t - 10.4(\Delta Gr_t + 1.17\Delta WA_t) + u_{1,t}, \tag{5}$$

where $u_{1,t}$ is stationary. This implies that the WAIS and GrIS mass changes are positively co-moving around a negatively sloped trend (-3.79 Gigatonnes of ice per month). The esti-

[8] Once the rank is imposed, we can test whether any of the ice sheets is an I(1) process using the multivariate test in Juselius (2014). The results in Appendix Table A.2 strongly indicate that these hypotheses are rejected.

[9] Doornik and Juselius (2018, Chapter 5) notes that identification of β in this context requires $r-1$ identifying restrictions on each of the vectors.

[10] The β and d coefficients are presented in error-correction form such that when interpreting the relationships, the signs need to be flipped for all but the normalized coefficients.

Table 3: The long-run structure for Model 1 ($r = 2, s_1 = 0, s_2 = 1$)

Test of over-identifying restriction on β : $\chi^2(1) = 1.13$ {0.29}					
		Gr_t	WA_t	EA_t	$trend/constant$
β_1'	x_t	-0.41 [-5.5]	1.00	0.00	3.79 [8.0]
d_1'	Δx_t	10.37 [4.4]	12.16 [1.9]	2.25 [0.4]	-2.09 [-1.2]
α_1		-0.006 [-2.7]	-0.003 [-1.8]	0.009 [4.3]	
β_2'	x_t	0.00	1.00	1.00	6.90 [16.0]
d_2'	Δx_t	-2.42 [-1.1]	52.86 [13.4]	45.14 [11.7]	-14.21 [-12.8]
α_2		-0.001 [-0.2]	-0.004 [-2.5]	-0.009 [-3.7]	
β_1'	Δx_t	-0.41	1.00	0.00	3.79
ζ_1		0.07 [1.8]	-0.02 [-0.6]	0.15 [3.8]	
β_2'	Δx_t	0.00	1.00	1.00	6.90
ζ_2		0.03 [0.3]	0.20 [2.6]	0.20 [1.9]	

Note: t-values in square brackets. p-values in squiggly brackets. β and d coefficients are in error-correction form. Signs need to be flipped to interpret relationships.

mated medium-run adjustment coefficients show simultaneous feedback dynamics among the ice sheets in all three regions. While the GrIS exhibits equilibrium-diverging behaviour, the WAIS is equilibrium-correcting. Thus, in the medium run, a reduction in Greenland mass balance (leading to a negative ice mass anomaly) driven by external forcing (the exogenous trend) positively feeds back with a stronger reduction in mass balance and so on. Such a feedback parallels physical processes such as ice-elevation and ice-albedo feedbacks (e.g. Pattyn, 2006). On the other hand, the statistically weak equilibrium-correcting effect for WAIS indicates a system that is less susceptible to internal feedbacks following a change in external forcing (i.e. ice-elevation and ice-albedo effects are limited for WAIS). This suggests that changes in the northern hemisphere are driving this relationship. The small, but insignificant explosive characteristic root in Table 2, indicates that the ice sheets could be near a tipping point in which the equilibrium-diverging behaviour of Greenland exceeds the equilibrium-correcting behaviour of West Antarctica.

We normalize the long-run intra-antarctic relationship on EA_t and rewrite it as:

$$EA_t = 14.2 - 6.9t - WA_t - 52.9(\Delta WA_t + 0.85\Delta EA_t) + u_{2,t}, \tag{6}$$

where $u_{2,t}$ is stationary. The sum of EA_t and WA_t are negatively co-moving (one is increasing while the other is decreasing) and the sum is developing around a negative trend ($-6.9t$) imply-

Table 4: The long-run structure for Model 2 ($r = 1, s_1 = 1, s_2 = 1$)

Test of over-identifying restriction on $\beta : \chi^2(1) = 0.00$ {0.99}					
		Gr_t	WA_t	EA_t	$trend/constant$
β_1'	x_t	-0.45 [-5.2]	1.00	0.0	3.52 [6.8]
d_1'	Δx_t	7.47 [1.3]	15.49 [1.4]	-1.18 [-1.2]	-3.44 [-0.9]
α_1		-0.007 [-3.2]	-0.004 [-2.6]	0.005 [2.3]	
		ΔGr	ΔWA	ΔEA	$constant$
β_1'	Δx_t	-0.45	1.00	0.00	3.52
ζ_1		0.10 [2.9]	-0.03 [-1.4]	-0.10 [-3.1]	
$\beta_{\perp 1}'$	Δx_t	0.163	0.002	1.00	0.020
ζ_2		*	*	-0.17 [-6.7]	

Note: t-values in square brackets. p-values in squiggly brackets. β and d coefficients are in error-correction form. Signs need to be flipped to interpret relationships.

ing that the total AIS mass anomaly is declining on average by 6.9 Gigatonnes per month. The estimates of d_2 and α_2 in Table 3 show that both EA_t and WA_t are equilibrium-correcting in the medium- and long-run, while the GrIS does not respond directly to this relation. However, the positive long-run relationship between Greenland and West Antarctica implies an indirect negative long-run relationship between Greenland and East Antarctica.

In the $I(2)$ model in (4), $\beta' x_t \sim I(1)$. Hence, $\beta' \Delta x_t \sim I(0)$ represents a change in the equilibrium divergence, the effect of which is given by the coefficient ζ the estimates of which are reported at the end of Table 3. They show that changes in the divergence from the bipolar relationship, $\beta_1' \Delta x_t$, have a small equilibrium-correcting effect on Greenland, do not seem to affect West Antarctica, and have a positive effect on East Antarctica. Thus, the equilibrium-diverging effects for Greenland are slightly offset by its positive response to changes in deviations from the equilibrium. The estimates of ζ_2 show that changes in the divergence from the intra-antarctic relationship, $\beta_2' \Delta x_t$, have no effect on Greenland whereas both West and East Antarctica diverge from them, which slows down how quickly they correct to the long-run equilibrium.

6.2 Model 2: I(2) with 1 Multi-Cointegrating Relation ($r = 1, s_1 = 1, s_2 = 1$)

We now consider the case of one multi-cointegrated relation. Table 4 reports the estimates of the multi-cointegrated relation, together with the long-run adjustment coefficients and the adjustment coefficients.[11] We interpret this as the bipolar relationship between Greenland and West Antarctica, which is identical to the corresponding relation discussed in Model 1. The one

[11] With the rank imposed, we can test whether any of the ice sheets is an I(1) process using the multivariate test in Juselius (2014). The results in Appendix Table A.2 strongly indicate that these hypotheses are rejected.

just-identifying zero restriction is not rejected based on $\chi^2(1) = 0.00[0.99]$.

If we impose the restrictions implied by the correlations between Greenland and West Antarctica and East and West Antarctica in Bamber and Aspinall (2013), then they are weakly rejected with a p-value of 0.09. As with Model 1, we find a weaker long-run relationship between West Antartica and Greenland than Bamber and Aspinall (2013) at about 0.45. Unlike Model 1, the estimated parameter is not dynamically stable; see panel B of Appendix Figure A.1.

The medium-run relation, $\beta'_{\perp,1}\Delta x_t$, is basically a unit vector in EA_t, implying that EA_t is possibly $I(1)$ rather than $I(2)$. The test of a unit vector in τ was not rejected based on $\chi^2(2) = 3.22[0.20]$. Of the estimated adjustment coefficients, only East Antarctica responds.

The estimates in Table 3 show that deviations from the long-run bipolar relationship, $\zeta'_1\beta_1\Delta x_t$, have an equilibrium-correcting effect on Greenland and West Antarctica and a negative effect on East Antarctica. Thus, as in Model 1, the equilibrium-diverging effects for Greenland are somewhat offset by its response to the change in deviations from the bipolar equilibrium.

The main difference between Model 1 and Model 2 is that in the latter case, East Antarctica is approximately $I(1)$ and is more or less detached from the influence of the other ice sheets in the medium- and long-run. This is consistent with the fact that East Antarctica is physically grounded and is therefore not as strongly influenced by changes in ocean and atmospheric temperatures that link Greenland and West Antarctica. This contrasts with Model 1 where the sum of EA_t and WA_t is $I(1)$ and EA_t corrects to deviations from the bipolar equilibrium. Figure 1 shows that through 2001, EA_t looked more like an $I(1)$ series. However, after 2001, it behaves more like an $I(2)$ series similar to the other ice sheets. Because the $I(1)$ behaviour is in the beginning of the period and the $I(2)$ behaviour is more recent, approximating EA_t with an $I(1)$ process may not be very good for the model's future performance. Furthermore, Johansen et al. (2010) and Di Iorio et al. (2016) show that even if a series is only near-$I(2)$ then it can be better to approximate it as $I(2)$.

6.3 Model 3: I(1) with 2 Cointegrating Relations ($r = 0, s_1 = 1, s_2 = 2$)

We consider the $I(1)$ model of ice mass balance, i.e. Δx_t. While this is the first case not to be rejected by the trace tests in Table 2, we view this case with some scepticism. This is partly because two $I(2)$ trends in the data is inconsistent with the number of near unit roots in the unrestricted model, partly because the remaining trace tests are consistent with one $I(2)$ trend, and finally because the trace tests in the $I(1)$ model for Δx_t (not reported) strongly rejected $r = 1$ (i.e. $s_1 = 1$) but did not reject $r = 2$ (i.e. $s_1 = 2$).

However, it is worth understanding what is lost by choosing a simpler model. If $\Pi = 0$ in

Table 5: The long-run structure of Model 3 ($r = 0, s_1 = 1, s_2 = 2$)

Test of over-identifying restriction on β:$\chi^2(1) = 4.44$ {0.04}				
	ΔGr	ΔWA_t	ΔEA_t	*const*
β_1'	-0.07 [-0.73]	1.00	0.00	6.39 [3.02]
α_1	0.01 [0.41]	-0.06 [-2.37]	0.13 [3.74]	
β_2'	0.00	1.00	1.00	5.78 [3.44]
α_2	-0.02 [-0.77]	-0.01 [-0.46]	-0.17 [-6.31]	

Note: t-values in square brackets. p-values in squiggly brackets. β coefficients are in error-correction form. Signs need to be flipped to interpret relationships.

(3), then Model 3 is the correct choice and so solving the reduced rank of $\Gamma = \alpha\beta'$ we would obtain estimates of the relevant long-run relations. But, the significant estimates of α and β in Models 1 and 2 suggest that $\Pi \neq 0$. Hence, by restricting $\Pi \equiv 0$, Model 3 is uninformative about the dynamic feedback between ice sheet mass anomaly in the $I(2)$ models. One may also ask whether the long-run equilibrium relationship in Model 3, $\Gamma\Delta x_t = \alpha\beta'\Delta x_t$, can be used to recover the medium-run changes to deviations from the long-run relationship in Model 1, $\xi\tau'\Delta x_t$, where $\tau' = [\beta_1, \beta_2]$. However, because $\Gamma\Delta x_t = \xi\tau'\Delta x_t + d'\Delta x_t$, the reduced rank of $\Gamma = \alpha\beta' \neq \xi\tau'$ when $\Pi \neq 0$ and $d \neq 0$. In that case, the $I(1)$ cointegration results based on ice sheet mass balance will differ from the $I(2)$ cointegration results based on ice sheet mass anomalies and will produce biased estimates of the long-run equilibrium relationships.

Table 5 reports the estimates of $\Gamma = \alpha\beta'$ subject to $\Pi \equiv 0$ in (3). The test of the same over-identifying restriction consistent with the hypotheses of the common GR/WA characteristic mass loss as in Model 1 is rejected based on $\chi^2(1) = 4.44[0.04]$. However, the two over-identifying restrictions implied by the correlations in Bamber and Aspinall (2013) are not rejected based on $\chi^2(2) = 1.23[0.54]$. Greenland is insignificant in the β_1 relation and while β_2 is similar to the β_2 relation in Model 1, it is completely "forced" by restrictions that were rejected. It is also unclear whether the equilibrium is correcting or diverging given that the adjustment dynamics are generally insignificant.

Together the results from the three models indicate that accumulating the mass balance data to get the $I(2)$ model is advisable when $\Pi \neq 0$. Furthermore, as long as East Antarctica is $I(2)$ or near-$I(2)$ then Model 1 is preferable to Model 2. That being said, the simpler models may be more useful for forecasting if the long-run relationships are subject to change.

7 Discussion and Interpretation of the I(2) System

By focusing on the $I(2)$ model with two multi-cointegrating relations as our preferred model of the sheet system we can now move on from model estimation and begin to interpret and evaluate its implications. We start in section 7.1 by examining the link between the stochastic $I(2)$ trend and other climate variables. Next, in section 7.2 we explore the dynamics of the $I(2)$ model by looking at how an abrupt change in the GrIS propagates through the system. In section 7.3 we perform an out-of-sample evaluation of how well the $I(2)$ and the other CVAR models perform against the most recent satellite observations. Finally, in section 7.4 we forecast the ice sheet contributions to sea-level rise through 2100.

7.1 Climate Drivers of the Stochastic I(2) Trend

It is possible to analyse the trend movements of the ice sheets by inverting the models into their moving average representations. For the purpose of this analysis, we focus exclusively on Model 1 since it is our preferred specification from the three considered above. The long-run dynamics of Model 1 are described by one stochastic $I(2)$ trend, $StI2_t$, one $I(1)$ trend, here $\Delta StI2_t = StI2_t - StI2_{t-1}$, a linear trend, and stochastic components:

$$\begin{bmatrix} Gr_t \\ WA_t \\ EA_t \end{bmatrix} = \begin{bmatrix} a_1 \\ a_2 \\ a_3 \end{bmatrix} StI2_t + \begin{bmatrix} b_1 \\ b_2 \\ b_3 \end{bmatrix} \Delta StI2_t + \begin{bmatrix} c_1 \\ c_2 \\ c_3 \end{bmatrix} t + stoch.comp. \tag{7}$$

where $StI2 = \alpha'_{\perp 2}\varepsilon_i$ and $\hat{\alpha}'_{\perp 2} = [\underset{(-2.65)}{1.116}, -1.0, \underset{(-1.74)}{-0.412}]$ where the numbers in parenthesis are t-statistics. The a coefficients are proportional to $\beta_{\perp 2}$, the b and c coefficients are not straightforward to estimate. Instead the estimates in Table 6 were calculated by simple regressions equation by equation. We note the following: (i) the single equation estimates of the $I(2)$ trend coefficients are quite close to the estimates of $\beta_{\perp 2}$ which were obtained from the system estimates of the moving average representation of Model 1, (ii) the coefficients of the stochastic $I(2)$, $I(1)$ and linear trends deviate a lot across the individual ice sheets, (iii) while the stochastic trends differ in sign between West and East Antarctica the linear trend has a negative coefficient in all three ice sheets.

The stochastic trends capture Greenland and West Antarctica well but not East Antarctica. In all three ice sheets, the residuals exhibit a pronounced persistence, which is because the stationary short-run dynamics were not included in the estimation; see Appendix Figure A.2.

The change in the stochastic trend closely follows the historical evolution of global ocean

Table 6: Estimated coefficients of the stochastic and linear trends in the data

	Gr	WA	EA
$\beta_{\perp 2}$	0.39	0.16	−0.16
Single equation regression estimates			
a	0.41	0.16	−0.13
b	0.64	−3.63	2.21
c	−2.72	−4.72	−1.60
Linear trend estimated by OLS			
	−11.53	−7.11	0.58

heat content, as measured by Cheng et al. (2017). The relationship is seen in Figure 3 and is estimated explicitly in Appendix Table A.3. Global ocean heat content is in turn linearly related to cumulative emissions; see for example Williams et al. (2012).

This explains why the stochastic trends capture changes in the Greenland and West Antarctic ice sheets but not East Antarctic. WAIS is susceptible to changes in ocean heat content because it is largely grounded below sea level with significant ice shelves buttressing it so that sub-marine melting leads to debuttressing, enhanced ice flow speeds, and in turn increased mass loss. On the other hand, GrIS mass loss is more sensitive to atmospheric surface temperature via SMB, and which is linked with ocean heat content via cumulative CO_2 emissions (Williams et al., 2012). The stochastic trends are less explanatory for changes in the EAIS where ocean heat content effects are largely offset by factors such as smaller ice shelves, colder surface air temperatures and increasing SMB. This asymmetry between mass changes of WAIS and EAIS is also linked to the pattern of regional atmosphere-ocean effects at the poles by global teleconnections that are primarily induced by anomalous warming of the tropics (Li et al., 2021).

Thus the stochastic trends capture the global ocean heat content (linked to Earth's energy imbalance and cumulative emissions) that serve to induce GrIS and WAIS mass loss. The co-movement between the stochastic trends in the ice sheets and global ocean heat content suggests that there could be additional interactions within the ice-sheet-ocean-atmosphere system (e.g., Bruns et al., 2020, Park et al., 2023, Li et al., 2021).

7.2 Dynamic Analysis of the Ice Sheet System

We can explore how abrupt changes propagate dynamically through the system of ice sheets. In particular, we examine how a sudden loss of ice in Greenland leads to mass changes across all three ice sheets. Using the preferred Model 1 with two multi-cointegrating relations, we shock the Greenland ice sheet at month 0 so that there is an immediate decline in ice mass acceleration by 1 $Gt/month^2$. The cumulative response to this change is then traced out through the model for five years (i.e. 60 months). This is akin to an impulse response function where we are

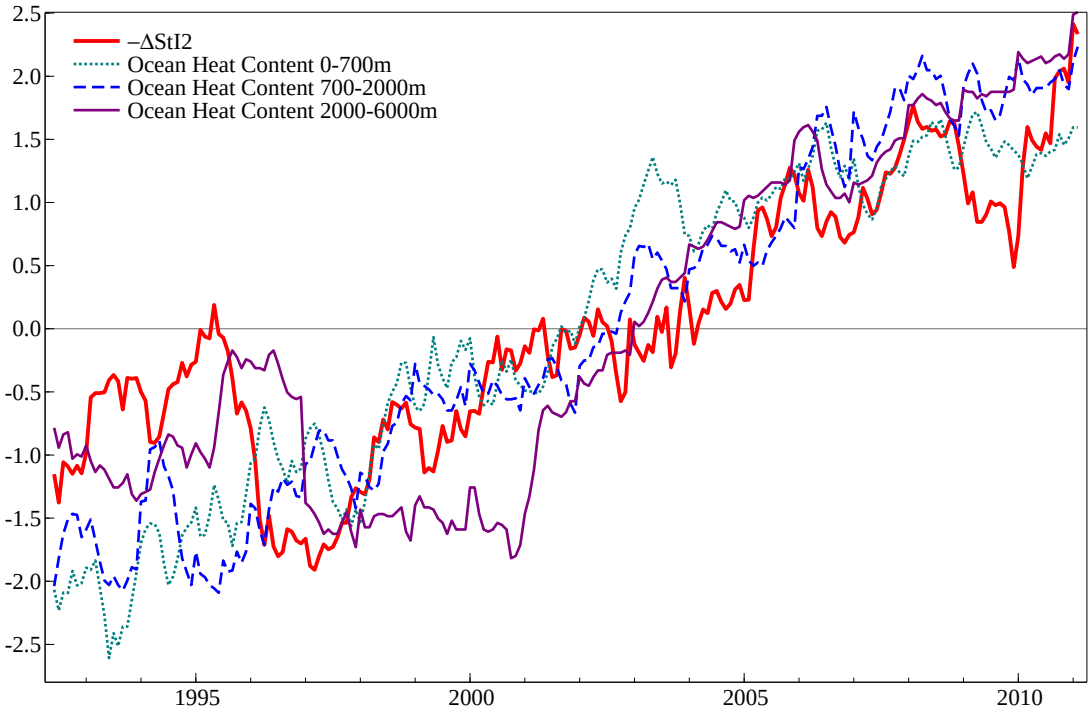

Note: All series are standardized to have zero mean and unit variance over the sample. Ocean heat content is rescaled to match the mean and ranges of the change in the stochastic ice loss trend.

Figure 3: Stochastic Ice Loss Trend and Ocean Heat Content from Cheng et al. (2017).

assuming a recursive Cholesky identification restriction in which Greenland is ordered last.[12]

Figure 4 shows the cumulative responses to this change on ice mass acceleration, mass balance, and mass anomalies in Greenland, West Antarctica and East Antarctica. The change in Greenland has lagged spillover effects into West and East Antarctica initially causing small accelerations in mass loss. Six months later, West Antarctica's mass loss acceleration becomes positive before becoming negative again after 18 months resulting in a gradual decline in ice sheet mass. For East Antarctica, the negative acceleration becomes positive after 12 months and remains so for the rest of the period resulting in a gradual increase in ice mass after 5 years. For Greenland, the negative shock is initially self-amplifying and the following decay fails to return to zero leading to persistent, increasing mass loss over time. This behaviour is consistent with instability within the system, akin to being near or having crossed a tipping point (or undergoing a tipping phase). While we do not explicitly test for the presence of a tipping point (or structural break) and are thus unable to estimate any exact timing of a tipping point, the explosive behaviour and lack of equilibrium-correction of the GrIS is consistent with being near (or undergoing) this transition. Future research could test for and explore these issues further.

The results of this exercise highlight three key features of the dynamics in the model. (i)

[12]Note that the residual correlation between Greenland and West Antarctica is large enough (-0.2) such that our identification assumption is nontrivial for West Antarctica for the first ten months following the shock.

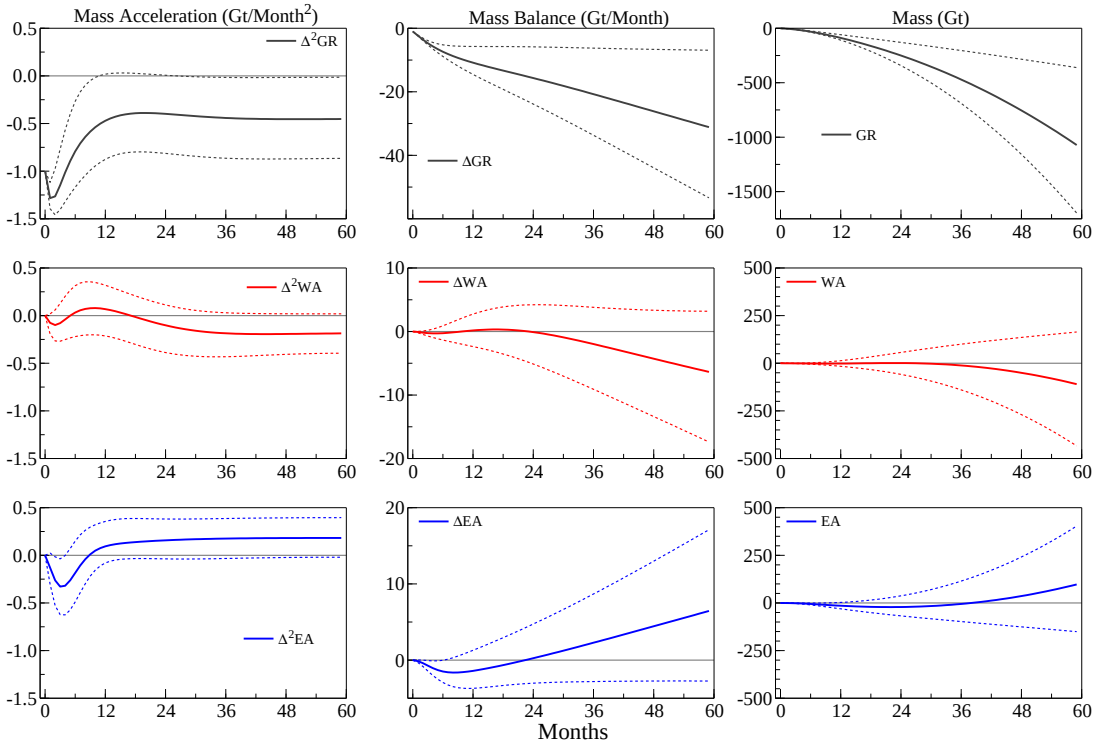

Note: Gt stands for Gigatonnes. The dotted bands represent the +/- 2σ confidence intervals which are derived based on 10,000 bootstrap draws of the estimated model residuals under the assumption that they are iid multivariate normal.

Figure 4: Cumulative Response to a 1 Gt Loss of Ice in Greenland

There is a persistent mass loss to WAIS and GrIS with a common trend that reflects a positive bipolar response to a common forcing and delayed feedbacks. We interpret this as primarily driven by ocean heat content where delayed feedbacks affect atmosphere-ocean circulation that propagate through to West Antarctica. (ii) There is a weak negative relationship between Greenland/West Antarctica and East Antarctica that reflects the relative insensitivity of East Antarctica to ocean heat content but responds indirectly through increased surface mass balance (leading to mass gain). The extent of a climate-induced response to East Antarctica is unclear in current physical models (e.g. Stokes et al., 2022) though as with Greenland and West Antarctica there is evidence of a threshold leading to forced behaviour. Our analysis indicates this hasn't yet been reached, unlike with the other ice sheets (Rignot et al., 2019). (iii) The equilibrium-diverging nature of GrIS highlights the risk of a complete loss of the ice sheet occurring about twice as fast as the most extreme estimates from coupled models (e.g., Lenton et al., 2008) and consistent with recent observations of Greenland being close to (or having crossed) a tipping point. This serves to illustrate the elevated sensitivity of the GrIS under extreme warming (Boers and Rypdal, 2021).

7.3 Evaluating the Models using Out-of-Sample Forecasts

In this subsection we compare the model forecasts against the most recent satellite observations available through early-2021 (which were not used for estimation) and against several simple baseline forecast models to evaluate their performance and to assess whether the in-sample results hold up over the most recent decade. We evaluate the CVAR model forecasts against a simple AR(12) model and against a VAR(1) model of $\Delta^2 x_t$, which implies that $\Pi = \Gamma = 0$ in (3).[13] We also consider alternative specifications of the CVAR models in which we relax the long-run over-identifying restrictions. Finally, we also transform the models to protect against shifts or changes in the equilibrium. To illustrate this robustification, consider the following representation of the $I(2)$ model:

$$\Delta^2 x_t = \alpha \mathrm{LR}_{t-1} + \zeta \mathrm{MR}_{t-1} + \Gamma_{12} \Delta^2 x_{t-1} + \Theta K_t + \epsilon_t, \tag{8}$$

where LR_{t-1} is the long-run equilibrium, MR_{t-1} is medium-run equilibrium, and K_t is a vector of seasonal and outlier dummies. The forecasts can be robustified following Hendry (2006) and Castle et al. (2015) by quasi-differencing (8) and ignoring any higher order terms

$$\Delta^2 x_t = \Delta^2 x_{t-1} + \alpha \Delta \mathrm{LR}_{t-1} + \zeta \Delta \mathrm{MR}_{t-1} + \tilde{\Theta} \tilde{K}_t + v_t. \tag{9}$$

This removes the equilibrium-mean from each of the terms. It is extended, following Castle and Kurita (2021), by smoothing over local estimates of the equilibrium-mean

$$\Delta^2 x_t = \frac{1}{w_1} \sum_{j=1}^{w_1} \Delta^2 x_{t-j} + \alpha \left\{ \mathrm{LR}_{t-1} - \frac{1}{w_2} \sum_{s=1}^{w_2} \mathrm{LR}_{t-1-s} \right\} + \zeta \left\{ \mathrm{MR}_{t-1} - \frac{1}{w_3} \sum_{q=1}^{w_3} \mathrm{MR}_{t-1-q} \right\} + ..., \tag{10}$$

where the first term is a local average acceleration rate of the system and the second and third terms are deviations from local estimates of the equilibrium long and medium-run means. Adaptive estimates of the equilibrium means help robustify the forecasts to abrupt changes in the long-run trend and mean that have occurred in-sample, especially at longer horizons; see Martinez et al. (2022). Castle et al. (2015) show that it can also help protect against model mis-specification. This is important since the ice sheets could be subject to instabilities and abrupt changes. We focus on the case where $w_1 = 1$ and $w_2 = w_3 = 36$ so that we smooth the estimates of the equilibria means over three years.[14]

Evaluation of the forecasts is complicated by limitations of available ice mass anomaly data

[13] A completely unrestricted VAR performs slightly worse than the restricted VAR for Greenland but slightly better for West and East Antarctica.

[14] Note that unlike Castle and Kurita (2021), we endogenise forecasts of the equilibria relationships.

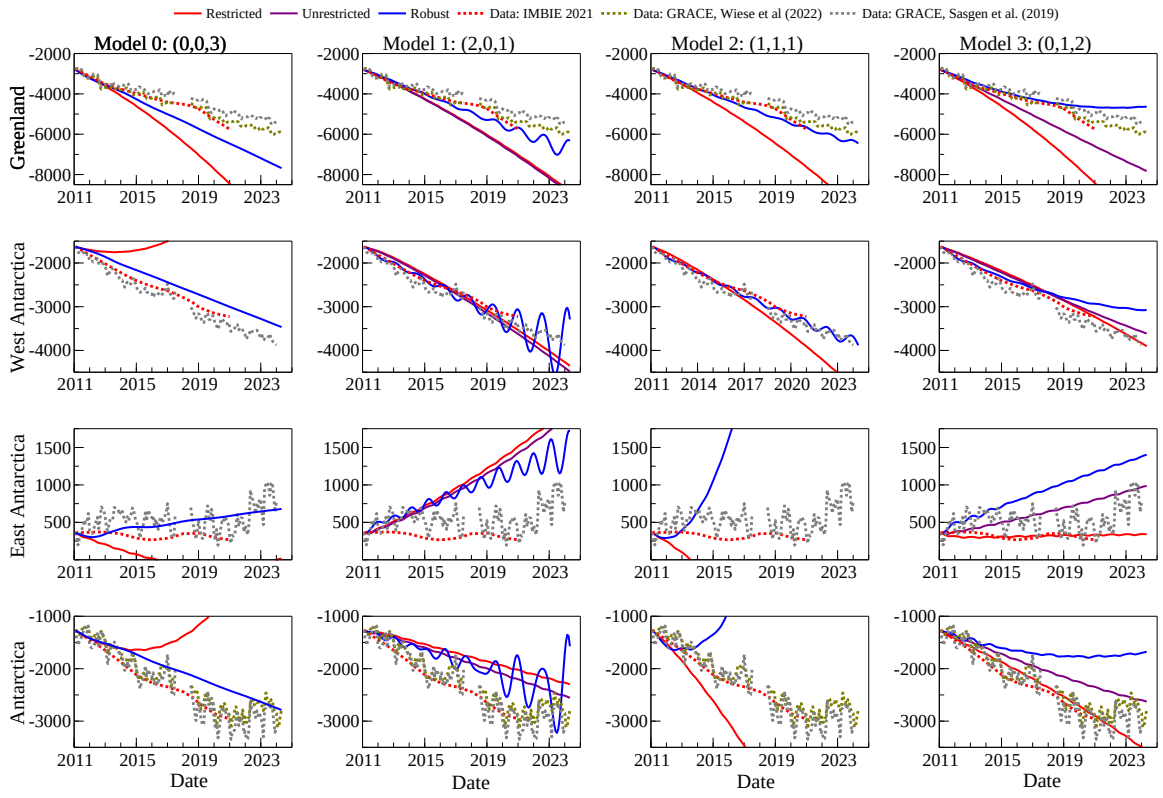

Note: Restricted, Unrestricted and Smooth Robust refer to the different specifications for each model forecast. Data are intercept corrected to match the last observation of the IMBIE data.

Figure 5: Alternative Forecasts of Ice Sheet Mass Anomalies (in Gt)

since the end of the original sample in 2011. Although updates to IMBIE since Shepherd et al. 2012 have remained at a monthly timescale, various smoothing approaches have been applied (12-36 months) to reconcile different instrumental measurements of ice mass anomalies and/or mass balance (e.g., Shepherd et al., 2018, 2019, 2021; Otosaka et al., 2023). Such smoothing removes much of the inter-annual variability that we seek to model making it unsuitable for direct use and merely intercomparison with forecasts.

An alternative data source is NASA's Gravity Recovery and Climate Experiment (GRACE), and Follow-On (GRACE-FO) missions, which also contributed to the IMBIE data products. This data runs from 2002 to present, but contains a 12-month gap (June 2017 - June 2018). Wiese et al. (2022) produce up-to-date estimates of ice sheet mass anomalies for Greenland and Antarctica available from NASA JPL's Physical Oceanography Distributed Archive Center. Alternatively, Sasgen et al. (2019) produce ice mass anomalies for GrIS, WAIS, and EAIS as well as their individual basins.

We present all three data measures in Figure 5. However, we focus on the Sasgen et al. (2019) measure in order to have the longest and most disaggregated sample possible. Each data series is intercept-corrected so that it is consistent with the original IMBIE data, however in general the GRACE data exhibit much greater monthly variability.

Table 7: Forecast Performance Relative to an AR(12) Model (Feb. 2011 - Dec. 2023) evaluated using GRACE/GRACE-FO mass anomalies from Sasgen et al. (2019)

	Greenland			**West Ant.**			**East Ant.**			**Joint**$^{\alpha}$		
	R	**Ur**	**Sr**	**R**	**Ur**	**Sr**	**R**	**Ur**	**Sr**	**R**	**Ur**	**Sr**
AR	1.00	1.00	0.33	1.00	1.00	0.43	1.00	1.00	1.01	1.00	1.00	0.57
M0	0.78	0.78	0.34	5.99	5.99	0.95	1.28	1.28	**0.42**	1.01	1.01	0.58
M1	**0.46**	0.48	0.22	**0.60**	**0.67**	0.67	1.64	1.49	1.16	**0.71**	0.69	0.59
M2	0.59	0.59	0.18	1.10	1.10	**0.33**	3.77	3.77	11.2	0.83	0.83	0.97
M3	0.77	**0.37**	**0.09**	0.65	0.70	1.01	**0.64**	**0.54**	1.08	0.96	**0.60**	**0.42**

Note: Performance is calculated as the square root of the average squared error from a single path of forecasts across all horizons and relative to the baseline model. The forecasts for July 2017 - May 2018 are omitted due to missing data. Bolded values indicate best performance. Models: AR: Baseline AR(12); M0: restricted VAR; M1 Model 1; M2 Model 2; M3 Model 3. R: Long-run over-identifying restrictions imposed. Ur: No Long-run over-identifying restrictions imposed. Sr: Smooth Robust Transformation with $w_1 = 1$ and $w_2 = w_3 = 36$.

$^{\alpha}$Calculated as the determinant of the system of ice sheets following Clements and Hendry (1993).

The data and forecasts from each model are presented in Figure 5. Each column of panels presents an alternative model and each row of panels represents an ice sheet. The panels show that the alternative measures of actual ice sheet mass anomalies are generally aligned. However, there are important differences between the GRACE and IMBIE measurements for East Antarctica such that GRACE is generally higher (see Shepherd et al., 2018).

There are also considerable differences between the model forecasts. The restricted VAR performs poorly except for Greenland and also when robustifying the forecasts. Model 1 generally captures the trends in the data albeit with a stronger downward trend for Greenland and a weaker trend for Antarctica. Model 2 performs reasonably well for Greenland and West Antarctica but does poorly for East Antarctica, which indicates that its $I(1)$ specification for East Antarctica is not correct. Model 3 over-predicts the trend in Greenland but over-shoots West Antarctica and under-shoots East Antarctica so that its overall path for Antarctica is relatively accurate. Relaxing the over-identifying restrictions does not substantially alter the forecasts from Model 1 but does improve the accuracy of Model 3. The smooth robust transformations generally improve the forecasts, especially for the simpler likely misspecified models.

Table 7 confirms these results. All of the CVAR models perform better than the baseline AR model except for in East Antarctica. Model 1 does best for Greenland, West Antarctica, and the joint system when imposing the over-identifying restrictions. This provides support for the bipolar and intra-antarctic long-run relationships embedded in Model 1 and provides evidence against treating East Antarctica as an $I(1)$ process as in Model 2 or imposing $\Pi \equiv 0$ as in Model 3. The best forecast for most of the ice sheets is obtained when relaxing the restrictions

and using smooth adaptive forecasts. This illustrates that Model 3 performs best for Greenland and the joint system, Model 2 is best for West Antarctica and the restricted VAR does best for East Antarctica. While Model 1 fits best with the restrictions, simpler models allow for greater flexibility without interpretability.[15]

7.4 Projecting Future Sea-Level Rise Contributions

We extend the ice sheet mass anomaly forecasts to 2100 and convert them into their global mean sea-level change equivalent (GMSLE, the global mean sea-level change occurring if the ice mass change were equally distributed across the global oceans) to compare with the IPCC's high emissions (SSP5-85)[16], medium confidence projections. Unlike IPCC's scenario-based approach, we generate true out-of-sample forecasts conditional on the estimated historical relationships and extrapolate the stochastic and linear trends. In this sense our approach here is similar to that used in Diebold and Rudebusch (2021) and Diebold et al. (2023). However, as demonstrated in section 7.1, the underlying stochastic trends are closely correlated with ocean heat content. Assuming ocean heat content continues this trajectory through the 21st century, it would be consistent with high-emissions scenarios (e.g., SSP5-85; Fox-Kemper et al., 2021, Jevrejeva et al., 2020) thus we compare our forecasts with comparable projections from physical process-based models (Fox-Kemper et al., 2021) and structured expert judgment (Bamber et al., 2019).

Using Model 1 and the unrestricted version of Model 3, we extend forecasts to 2100. We then convert our forecasts of ice mass anomalies into GMSLE in 2100 relative to the mass averaged from 2002-2008 (the centre of the IPCC's reference time period), where 360 Gt mass loss $\approx$ 0.001 m GMSLE rise.

Figure 6 shows the forecasts of contributions to sea-level rise are at the high end of the IPCC medium confidence high-end projection for Greenland. Model 1 (0.20 - 0.35 m GMSLE) lies above the IPCC range (0.09-0.18 m GMSLE) though it exhibits less uncertainty than Model 3 (0.19 - 0.54 m GMSLE). This indicates that there is a risk of Greenland contributing even more than expected to sea-level rise if the long-run dynamics estimated in our models persist. This is more clearly the case when comparing with Bamber et al. (2019), where agreement is stronger (their range is 0.07-0.31 m GMSLE). Their incorporation of multi-level correlations of processes between ice sheets and structured expert judgement is reflected in a wider range and asymmetrical uncertainty (their median is 0.13 m GMSLE). The long-run dynamics indicates greater sensitivity than these two assessments presume.

The forecasts of Antarctica captured within the models are more mixed: Model 3 (0.06 - 0.22

[15]The results for the extended IMBIE data are very similar. See Appendix Table A.4.
[16]SSP: Shared Socio-economic Scenario; Riahi et al. (2017)

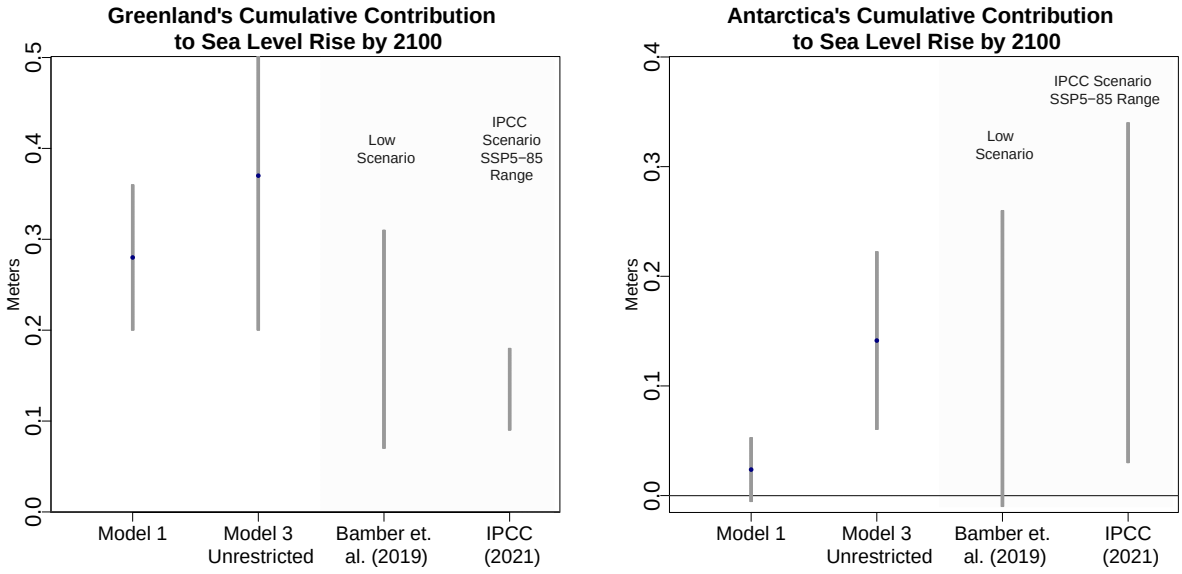

Note: Calculated as the forecast of ice sheet mass anomaly at the beginning of 2100 relative to average in 2002-2008 divided by 360,000 to account for ocean surface area and to convert from Gigatonnes into meters of global mean sea-level rise. Model 1 refers to the $I(2)$ rank 2 model and Model 3 Unrestricted refers to the $I(1)$ model without any over-identifying restrictions. The grey bars represent the +/- 1 s.d. forecast and parameter estimation uncertainty for the model forecasts and the likely range (the 17th-83rd percentile) for the expert judgement forecasts and the IPCC extreme climate change (scenario SSP5- 85) projections.

Figure 6: Modelled and published projections of GrIS and whole Antarctic Ice Sheet contributions to Global Mean sea-level rise by 2100 relative to 2002-2008 average.

m GMSLE) lies within the IPCC range (0.03-0.34 m GMLSE) while Model 1, which expects East Antarctica to continue to gain mass, is at the very low end (-0.04 - 0.08 m GMSLE). Such results are compatible with physical process-modelling studies that find the projected contribution of West Antarctica will increase through time due to it's inherent instability, whilst East Antarctica could contribute negatively (i.e. mass gain) or positively depending upon the competing processes of dynamic ice loss and snowfall accumulation (e.g., Bamber et al., 2018; Edwards et al., 2021; Stokes et al., 2022). Bamber et al. (2019) show similar ranges to both IPCC and our estimated models (their range is -0.1-0.26 m GMLSE). Likewise, expert judgement remains mixed on whether East Antarctica in particular will gain or lose mass over the century (Bamber et al., 2019; Fox-Kemper et al., 2021). Overall, our results indicate both wider uncertainties and higher GMSLE contributions than the medium confidence IPCC projections but do agree with low confidence projections that incorporate additional physical-process instabilities and expert judgement (Fox-Kemper et al., 2021).[17]

These results highlight the importance of improving the characterisation of co-variability of the contiguous ice sheet's mass change. The implications for reducing uncertainty of these processes and by extension global (and in fact regional) sea-level projections are significant.

[17]Note that long-range forecasts from simpler models than those considered here produce physically unrealistic results; e.g. see Appendix Figure A.3.

Estimates of coastal damages vary substantially (e.g., Hallegatte et al., 2013, Hinkel et al., 2014, Jevrejeva et al., 2018) and while economic growth in these models typically dominates damages, the effect of sea-level rise is not insubstantial. For example, Jevrejeva et al. (2018) showed that an 0.11 m increase in global mean sea level by 2100 translated into an additional US$ 1.4 trillion per year (0.25% of global GDP) of damages. Clearly adaptation to future sea-level rise will substantially reduce potential damages (e.g., Jevrejeva et al., 2018), but given the time scale of major coastal adaptation interventions can be up to 30 years (for example the Thames Barrier, London, UK), reducing the uncertainty of projections at any point in time will aid those making decisions (e.g. Oddo et al., 2020, Rasmussen et al., 2020).

8 Conclusion

In this paper we examine ice sheet dynamics and explicitly model the inter-dependence of the polar ice sheets, which have exhibited non-stationary changes over the recent record. Doing so allows us to analyse the dynamic interactions and feedback between the polar ice sheets using a statistical model and to test for and impose restrictions on these relationships that are consistent with existing physical and empirical models. We find that modelling the system as an $I(2)$ process with two multi-cointegrating vectors is both supported by the data and has a clear physical interpretation of one bipolar relationship between Greenland and West Antarctica driven by global ocean temperatures and one intra-antarctic relationship between West and East Antarctic which captures local climate conditions.

Using this general formulation we test for several alternative restrictions and specifications. We show that simple correlations are misleading and likely invalid for the non-stationary processes that describe ice sheet dynamics. Second, we assess whether the intra-antarctic relationship can be relaxed such that East Antarctica is actually an $I(1)$ process. While there is some support for this restriction in-sample given the earlier behaviour of East Antarctica prior to 2001, it is not supported out-of-sample causing the forecasts to be inaccurate. Finally, we evaluate whether the system can be simplified by treating the system as $I(1)$ in differences. In this setup, information is lost when imposing this restriction such that the bipolar relationship disappears and the ice sheets do not respond to one another in the medium-term. This is also apparent in the poor out-of-sample forecast performance of the restricted $I(1)$ model.

We analyse the dynamics of the system and show that the estimated stochastic trends are closely related to trends in ocean heat content. This illustrates that in future research the system of ice sheets could be embedded within a larger econometric model of the climate system (Bruns et al., 2020) or could be used to make conditional forecasts based on alternative

temperature and CO_2 pathways. We also explore how changes in the individual ice sheets propagate through the joint system and potential instabilities in the Greenland ice sheet that may lead to self-reinforcing feedback loops.

Our long-term projections of the polar ice sheet contributions to sea-level rise illustrate the risks from the estimated feedback loops. Our projections indicate that Greenland's contribution to sea-level rise could exceed the IPCC's likely range by around 50% by the end of the century and contribute more than 0.4 m to global mean sea-level rise. While this may be viewed as a pessimistic scenario, it illustrates that incorporating the dynamic interactions between the ice sheets within a statistical model and relating them to known physical processes allows us to better capture and understand the possibility of future risks due to climate change.

Acknowledgements

Funding to support this research was obtained from the Robertson Foundation (Grant number: 9907422). Earlier versions of this work benefited from helpful comments and discussions by participants at the European Geoscience Union General Assembly, the World Conference of Environmental and Resource Economics, and the Conference on Econometric Models of Climate Change. The paper also benefited from discussions with Jennifer Castle, Jurgen Doornik, Neil Ericsson, David Hendry, Stew Jamieson, Bent Nielsen, and Chris Stokes. Thanks to the handling editor Eric Hillebrand and also to two anonymous referees for their helpful comments. The views expressed here are solely those of the authors and do not necessarily represent those of the U.S. Department of the Treasury or the U.S. Government.

References

Bamber, J. L. and Aspinall, W. (2013). An expert judgement assessment of future sea level rise from the ice sheets. *Nature Climate Change*, 3(4):424–427.

Bamber, J. L., Oppenheimer, M., Kopp, R. E., Aspinall, W. P., and Cooke, R. M. (2019). Ice sheet contributions to future sea-level rise from structured expert judgment. *Proceedings of the National Academy of Sciences*, 116(23):11195–11200.

Bamber, J. L., Westaway, R. M., Marzeion, B., and Wouters, B. (2018). The land ice contribution to sea level during the satellite era. *Environmental Research Letters*, 13(6):063008.

Barletta, V. R., Sørensen, L. S., and Forsberg, R. (2013). Scatter of mass changes estimates at basin scale for Greenland and Antarctica. *Cryosphere*, 7:1411–1432.

Boers, N. and Rypdal, M. (2021). Critical slowing down suggests that the western greenland ice sheet is close to a tipping point. *Proceedings of the National Academy of Sciences*, 118(21):e2024192118.

Bruns, S. B., Csereklyei, Z., and Stern, D. I. (2020). A multicointegration model of global climate change. *Journal of Econometrics*, 214(1):175–197.

Castle, J. L., Clements, M. P., and Hendry, D. F. (2015). Robust approaches to forecasting. *International Journal of Forecasting*, 31(1):99–112.

Castle, J. L. and Kurita, T. (2021). A dynamic econometric analysis of the dollar-pound exchange rate in an era of structural breaks and policy regime shifts. *Journal of Economic Dynamics and Control*, 128(104139).

Chen, X., Zhang, X., Church, J. A., Watson, C. S., King, M. A., Monselesan, D., Legresy, B., and Harig, C. (2017). The increasing rate of global mean sea-level rise during 1993–2014. *Nature Climate Change*, 7(7):492.

Cheng, L., Trenberth, K. E., Fasullo, J., Boyer, T., Abraham, J., and Zhu, J. (2017). Improved estimates of ocean heat content from 1960 to 2015. *Science Advances*, 3(3):e1601545.

Church, J. A., Clark, P. U., Cazenave, A., Gregory, J. M., Jevrejeva, S., Levermann, A., Merrifield, M. A., Milne, G. A., Nerem, R. S., Nunn, P. D., Payne, A., Pfeffer, W., Stammer, D., and Unnikrishnan, A. (2013). Sea level change supplementary material. In Stocker, T., Qin, D., Plattner, G.-K., Tignor, M., Allen, S., Boschung, J., Nauels, A., Xia, Y., Bex, V., and Midgley, P., editors, *Climate Change 2013: The Physical Science Basis. Contribution of Working Group I to the Fifth Assessment Report of the Intergovernmental Panel on Climate Change*, chapter 13. Intergovernmental Panel on Climate Change.

Clem, K. R., Fogt, R. L., Turner, J., Lintner, B. R., Marshall, G. J., Miller, J. R., and Renwick, J. A. (2020). Record warming at the South Pole during the past three decades. *Nature Climate Change*, 10(8):762–770.

Clements, M. P. and Hendry, D. F. (1993). On the limitations of comparing mean square forecast errors. *Journal of Forecasting*, 12(8):617–637.

Coulombe, P. G. and Göbel, M. (2021). Arctic amplification of anthropogenic forcing: A vector autoregressive analysis. *Journal of Climate*, 34(13):5523–5541.

DeConto, R. M. and Pollard, D. (2016). Contribution of Antarctica to past and future sea-level rise. *Nature*, 531(7596):591.

DeConto, R. M., Pollard, D., Alley, R. B., Velicogna, I., Gasson, E., Gomez, N., Sadai, S., Condron, A., Gilford, D. M., Ashe, E. L., et al. (2021). The Paris Climate Agreement and future sea-level rise from Antarctica. *Nature*, 593(7857):83–89.

Di Iorio, F., Fachin, S., and Lucchetti, R. (2016). Can you do the wrong thing and still be right? Hypothesis testing in I(2) and near-I(2) cointegrated VARs. *Applied Economics*, 48(38):3665–3678.

Dickey, D. A. and Fuller, W. A. (1979). Distribution of the estimators for autoregressive time series with a unit root. *Journal of the American Statistical Association*, 74(366a):427–431.

Diebold, F. X. and Rudebusch, G. D. (2021). Probability assessments of an ice-free Arctic: Comparing statistical and climate model projections. *Journal of Econometrics*.

Diebold, F. X., Rudebusch, G. D., Göbel, M., Coulombe, P. G., and Zhang, B. (2023). When will arctic sea ice disappear? projections of area, extent, thickness, and volume. *Journal of Econometrics*, 236(2):105479.

Dietz, S., Rising, J., Stoerk, T., and Wagner, G. (2021). Economic impacts of tipping points in the climate system. *Proceedings of the National Academy of Sciences*, 118(34):e2103081118.

Dinniman, M. S., Klinck, J. M., and Hofmann, E. E. (2012). Sensitivity of circumpolar deep water transport and ice shelf basal melt along the West Antarctic Peninsula to changes in the winds. *Journal of Climate*, 25(14):4799–4816.

Doornik, J. A. (2009). Autometrics. In Shephard, N. and Castle, J. L., editors, *The Methodology and Practice of Econometrics: A Festschrift in Honour of David F. Hendry*, chapter 4, pages 88–121. Oxford: Oxford University Press.

Doornik, J. A. (2017). Maximum likelihood estimation of the I(2) model under linear restrictions. *Econometrics*, 5(2):1–20.

Doornik, J. A. and Juselius, K. (2018). *Cointegration Analysis of Time Series using CATS 3 for OxMetrics*. Timberlake Consultants Ltd.

Edwards, T. L., Brandon, M. A., Durand, G., Edwards, N. R., Golledge, N. R., Holden, P. B., Nias, I. J., Payne, A. J., Ritz, C., and Wernecke, A. (2019). Revisiting Antarctic ice loss due to marine ice-cliff instability. *Nature*, 566(7742):58.

Edwards, T. L., Nowicki, S., Marzeion, B., Hock, R., Goelzer, H., Seroussi, H., Jourdain, N. C., Slater, D. A., Turner, F. E., Smith, C. J., et al. (2021). Projected land ice contributions to twenty-first-century sea level rise. *Nature*, 593(7857):74–82.

Engle, R. F. and Granger, C. W. (1987). Co-integration and error correction: representation, estimation, and testing. *Econometrica*, pages 251–276.

Fox-Kemper, B., Hewitt, H. T., Xiao, C., Aedhalgeirsdóttir, G., Drijfhout, S. S., Edwards, T. L., Golledge, N. R., Hemer, M., Kopp, R. E., Krinner, G., et al. (2021). Ocean, cryosphere, and sea level change. In *Climate Change 2021: The Physical Science Basis. Contribution of Working Group I to the Sixth Assessment Report of the Intergovernmental Panel on Climate Change*, pages 1211–1361. Cambridge University Press.

Golledge, N. R., Keller, E. D., Gomez, N., Naughten, K. A., Bernales, J., Trusel, L. D., and Edwards, T. L. (2019). Global environmental consequences of twenty-first-century ice-sheet melt. *Nature*, 566(7742):65.

Granger, C. W. J. and Lee, T.-H. (1989). Investigation of production, sales and inventory relationships using multicointegration and non-symmetric error correction models. *Journal of Applied Econometrics*, 4(S1).

Grinsted, A., Bamber, J., Bingham, R., Buzzard, S., Nias, I., Ng, K., and Weeks, J. (2022). The transient sea level response to external forcing in cmip6 models. *Earth's Future*, 10(10):e2022EF002696. e2022EF002696 2022EF002696.

Hallegatte, S., Green, C., Nicholls, R. J., and Corfee-Morlot, J. (2013). Future flood losses in major coastal cities. *Nature climate change*, 3(9):802–806.

Hanna, E., Cappelen, J., Fettweis, X., Mernild, S., Mote, T., Mottram, R., Steffen, K., Ballinger, T., and Hall, R. (2021). Greenland surface air temperature changes from 1981 to 2019 and implications for ice-sheet melt and mass-balance change. *International Journal of Climatology*, 41(Suppl. 1):E1336–E1352.

Hanna, E., Pattyn, F., Navarro, F., Favier, V., Goelzer, H., van den Broeke, M. R., Vizcaino, M., Whitehouse, P. L., Ritz, C., Bulthuis, K., and Smith, B. (2020). Mass balance of the ice sheets and glaciers–progress since AR5 and challenges. *Earth-Science Reviews*, 201:102976.

Hanna, E., Topál, D., Box, J. E., Buzzard, S., Christie, F. D., Hvidberg, C., Morlighem, M., De Santis, L., Silvano, A., Colleoni, F., et al. (2024). Short-and long-term variability of the antarctic and greenland ice sheets. *Nature Reviews Earth & Environment*, 5(3):193–210.

Hendry, D. F. (2006). Robustifying forecasts from equilibrium-correction systems. *Journal of Econometrics*, 135(1-2):399–426.

Hendry, D. F. and Juselius, K. (2001). Explaining cointegration analysis: Part II. *Energy Journal*, 22(1):75–120.

Hinkel, J., Lincke, D., Vafeidis, A. T., Perrette, M., Nicholls, R. J., Tol, R. S., Marzeion, B., Fettweis, X., Ionescu, C., and Levermann, A. (2014). Coastal flood damage and adaptation costs under 21st century sea-level rise. *Proceedings of the National Academy of Sciences*, 111(9):3292–3297.

Hofer, S., Tedstone, A. J., Fettweis, X., and Bamber, J. L. (2017). Decreasing cloud cover drives the recent mass loss on the Greenland Ice Sheet. *Science Advances*, 3(6):e1700584.

Hoover, K. D., Johansen, S., and Juselius, K. (2008). Allowing the data to speak freely: The macroeconometrics of the cointegrated vector autoregression. *American Economic Review*, 98(2):251–255.

Humbert, A., Gross, D., Müller, R., Braun, M., Van De Wal, R., Van Den Broeke, M., Vaughan, D., and Van De Berg, W. (2010). Deformation and failure of the ice bridge on the Wilkins Ice Shelf, Antarctica. *Annals of Glaciology*, 51(55):49–55.

Jevrejeva, S., Jackson, L., Grinsted, A., Lincke, D., and Marzeion, B. (2018). Flood damage costs under the sea level rise with warming of 1.5 c and 2 c. *Environmental Research Letters*, 13(7):074014.

Jevrejeva, S., Palanisamy, H., and Jackson, L. (2020). Global mean thermosteric sea level projections by 2100 in CMIP6 climate models. *Environmental Research Letters*, 16(1):014028.

Johansen, S. (1988). Statistical analysis of cointegration vectors. *Journal of Economic Dynamics and Control*, 12(2-3):231–254.

Johansen, S. (1997). Likelihood analysis of the I(2) model. *Scandinavian Journal of Statistics*, 24(4):433–462.

Johansen, S. (1998). *Likelihood-based Inference in Cointegrated Vector Autoregressive Models*. Advanced Texts in Econometrics. Oxford University Press.

Johansen, S. (2006). Statistical analysis of hypotheses on the cointegrating relations in the I(2) model. *Journal of Econometrics*, 132(1):81–115.

Johansen, S. (2012). The analysis of nonstationary time series using regression, correlation and cointegration. *Contemporary Economics*, 6(2):40–57.

Johansen, S. and Juselius, K. (1990). Maximum likelihood estimation and inference on cointegration with applications to the demand for money. *Oxford Bulletin of Economics and statistics*, 52(2):169–210.

Johansen, S., Juselius, K., Frydman, R., and Goldberg, M. (2010). Testing hypotheses in an I(2) model with piecewise linear trends. An analysis of the persistent long swings in the DMK$ rate. *Journal of Econometrics*, 158(1):117–129.

Joughin, I. and Alley, R. B. (2011). Stability of the West Antarctic ice sheet in a warming world. *Nature Geoscience*, 4(8):506.

Juselius, K. (2006). *The Cointegrated VAR model: Methodology and Applications*. Advanced Texts in Econometrics. Oxford University Press.

Juselius, K. (2014). Testing for near I(2) trends when the signal-to-noise ratio is small. *Economics*, 8(1):1–22.

Juselius, K. and Assenmacher, K. (2017). Real exchange rate persistence and the excess return puzzle: The case of Switzerland versus the US. *Journal of Applied Econometrics*, 32(6):1145–1155.

Kaufmann, R. K. and Juselius, K. (2013). Testing hypotheses about glacial cycles against the observational record. *Paleoceanography*, 28(1):175–184.

Khan, S. A., Kjær, K. H., Bevis, M., Bamber, J. L., Wahr, J., Kjeldsen, K. K., Bjørk, A. A., Korsgaard, N. J., Stearns, L. A., Van Den Broeke, M. R., et al. (2014). Sustained mass loss of the northeast Greenland ice sheet triggered by regional warming. *Nature Climate Change*, 4(4):292–299.

King, M. D., Howat, I. M., Jeong, S., Noh, M. J., Wouters, B., Noël, B., and Broeke, M. R. (2018). Seasonal to decadal variability in ice discharge from the Greenland Ice Sheet. *The Cryosphere*, 12(12):3813–3825.

Kopp, R. E., Horton, R. M., Little, C. M., Mitrovica, J. X., Oppenheimer, M., Rasmussen, D., Strauss, B. H., and Tebaldi, C. (2014). Probabilistic 21st and 22nd century sea-level projections at a global network of tide-gauge sites. *Earth's Future*, 2(8):383–406.

Le Bars, D. (2018). Uncertainty in sea level rise projections due to the dependence between contributors. *Earth's Future*, 6(9):1275–1291.

Lenton, T. M., Held, H., Kriegler, E., Hall, J. W., Lucht, W., Rahmstorf, S., and Schellnhuber, H. J. (2008). Tipping elements in the earth's climate system. *Proceedings of the National Academy of Sciences*, 105(6):1786–1793.

Li, X., Cai, W., Meehl, G. A., Chen, D., Yuan, X., Raphael, M., Holland, D. M., Ding, Q., Fogt, R. L., Markle, B. R., et al. (2021). Tropical teleconnection impacts on antarctic climate changes. *Nature Reviews Earth & Environment*, 2(10):680–698.

Lim, Y.-K., Schubert, S. D., Nowicki, S. M., Lee, J. N., Molod, A. M., Cullather, R. I., Zhao, B., and Velicogna, I. (2016). Atmospheric summer teleconnections and Greenland Ice Sheet surface mass variations: Insights from MERRA-2. *Environmental Research Letters*, 11(2):024002.

Martinez, A. B., Castle, J. L., and Hendry, D. F. (2022). Smooth robust multi-horizon forecasts. *Advances in Econometrics: Essays in Honor of M. Hashem Pesaran, Prediction and Macro Modeling*, 43:143–165.

Mikkelsen, T. B., Grinsted, A., and Ditlevsen, P. (2018). Influence of temperature fluctuations on equilibrium ice sheet volume. *The Cryosphere*, 12(1):39–47.

Mouginot, J., Rignot, E., Bjørk, A. A., van den Broeke, M., Millan, R., Morlighem, M., Noël, B., Scheuchl, B., and Wood, M. (2019). Forty-six years of Greenland Ice Sheet mass balance from 1972 to 2018. *Proceedings of the National Academy of Sciences*, 116(19):9239–9244.

Nielsen, B. (2001). The asymptotic distribution of unit root tests of unstable autoregressive processes. *Econometrica*, 69(1):211–219.

Nielsen, B. (2006). Order determination in general vector autoregressions. *IMS Lecture Notes-Monograph Series Time Series and Related Topics*, 52(2006):93–112.

Nielsen, H. B. and Rahbek, A. (2007). The likelihood ratio test for cointegration ranks in the I(2) model. *Econometric Theory*, 23(4):615–637.

Oddo, P. C., Lee, B. S., Garner, G. G., Srikrishnan, V., Reed, P. M., Forest, C. E., and Keller, K. (2020). Deep uncertainties in sea-level rise and storm surge projections: Implications for coastal flood risk management. *Risk Analysis*, 40(1):153–168.

Oppenheimer, M., Glovovic, B., Hinkel, J., van de Wal, R., Magnan, A. K., Abd-Elgawad, A., Cai, R., Cifuentes-Jara, M., Deconto, R. M., Ghosh, T., Hay, J., Isla, F., Marzeion, B., Meyssignac, B., and Sebesvari, Z. (2019). Sea level rise and implications for low-lying islands, coasts and commnities. In Pörtner, H.-O., Roberts, D., Masson-Delmotte, V., Zhai, P., Tignor, M., Poloczanska, E., Mintenbeck, K., Alegría, A., Nicolai, M., Okem, A., Petzold, J., Rama, B., and Weyer, N., editors, *IPCC Special Report on the Ocean and Cryosphere in a Changing Climate*, chapter 4. The Intergovernmental Panel on Climate Change.

Oppenheimer, M., Little, C. M., and Cooke, R. M. (2016). Expert judgement and uncertainty quantification for climate change. *Nature Climate Change*, 6(5):445–451.

Otosaka, I. N., Shepherd, A., Ivins, E. R., Schlegel, N.-J., Amory, C., van den Broeke, M. R., Horwath, M., Joughin, I., King, M. D., Krinner, G., Nowicki, S., Payne, A. J., Rignot, E., Scambos, T., Simon, K. M., Smith, B. E., Sørensen, L. S., Velicogna, I., Whitehouse, P. L., A, G., Agosta, C., Ahlstrøm, A. P., Blazquez, A., Colgan, W., Engdahl, M. E., Fettweis, X., Forsberg, R., Gallée, H., Gardner, A., Gilbert, L., Gourmelen, N., Groh, A., Gunter, B. C., Harig, C., Helm, V., Khan, S. A., Kittel, C., Konrad, H., Langen, P. L., Lecavalier, B. S., Liang, C.-C., Loomis, B. D., McMillan, M., Melini, D., Mernild, S. H., Mottram, R., Mouginot, J., Nilsson, J., Noël, B., Pattle, M. E., Peltier, W. R., Pie, N., Roca, M., Sasgen, I., Save, H. V., Seo, K.-W., Scheuchl, B., Schrama, E. J. O., Schröder, L., Simonsen, S. B., Slater, T., Spada, G., Sutterley, T. C., Vishwakarma, B. D., van Wessem, J. M., Wiese, D., van der Wal, W., and Wouters, B. (2023). Mass balance of the greenland and antarctic ice sheets from 1992 to 2020. *Earth System Science Data*, 15(4):1597–1616.

Park, J.-Y., Schloesser, F., Timmermann, A., Choudhury, D., Lee, J.-Y., and Nellikkattil, A. B. (2023). Future sea-level projections with a coupled atmosphere-ocean-ice-sheet model. *Nature Communications*, 14(1):636.

Pattyn, F. (2006). GRANTISM: An Excel model for Greenland and Antarctic ice-sheet response to climate changes. *Computers & Geosciences*, 32(3):316–325.

Pattyn, F., Ritz, C., Hanna, E., Asay-Davis, X., DeConto, R., Durand, G., Favier, L., Fettweis, X., Goelzer, H., Golledge, N. R., et al. (2018). The Greenland and Antarctic ice sheets under 1.5 C global warming. *Nature Climate Change*, 8(12):1053–1061.

Post, E., Alley, R. B., Christensen, T. R., Macias-Fauria, M., Forbes, B. C., Gooseff, M. N., Iler, A., Kerby, J. T., Laidre, K. L., Mann, M. E., et al. (2019). The polar regions in a 2 C warmer world. *Science Advances*, 5(12):eaaw9883.

Pretis, F. (2020). Econometric modelling of climate systems: The equivalence of energy balance models and cointegrated vector autoregressions. *Journal of Econometrics*, 214(1):175–197.

Rasmussen, D., Buchanan, M. K., Kopp, R. E., and Oppenheimer, M. (2020). A flood damage allowance framework for coastal protection with deep uncertainty in sea level rise. *Earth's Future*, 8(3):e2019EF001340.

Riahi, K., Van Vuuren, D. P., Kriegler, E., Edmonds, J., O'neill, B. C., Fujimori, S., Bauer, N., Calvin, K., Dellink, R., Fricko, O., et al. (2017). The shared socioeconomic pathways and their energy, land use, and greenhouse gas emissions implications: An overview. *Global Environmental Change*, 42:153–168.

Rignot, E., Casassa, G., Gogineni, P., Krabill, W., Rivera, A., and Thomas, R. (2004). Accelerated ice discharge from the Antarctic Peninsula following the collapse of Larsen B ice shelf. *Geophysical Research Letters*, 31(18).

Rignot, E., Mouginot, J., Scheuchl, B., van den Broeke, M., van Wessem, M. J., and Morlighem, M. (2019). Four decades of Antarctic Ice Sheet mass balance from 1979–2017. *Proceedings of the National Academy of Sciences*, 116(4):1095–1103.

Sasgen, I., Groh, A., and Horwarth, M. (2019). GravIS RL06 Ice-Mass Change Products. V. 0002. GFZ Data Services at https://doi.org/10.5880/gfz.gravis_06_l3_ice, GFZ.

Schmith, T., Johansen, S., and Thejll, P. (2012). Statistical analysis of global surface temperature and sea level using cointegration methods. *Journal of Climate*, 25(22):7822–7833.

Seroussi, H., Pelle, T., Lipscomb, W. H., Abe-Ouchi, A., Albrecht, T., Alvarez-Solas, J., Asay-Davis, X., Barre, J.-B., Berends, C. J., Bernales, J., Blasco, J., Caillet, J., Chandler, D. M., Coulon, V., Cullather, R., Dumas, C., Galton-Fenzi, B. K., Garbe, J., Gillet-Chaulet, F., Gladstone, R., Goelzer, H., Golledge, N., Greve, R., Gudmundsson, G. H., Han, H. K., Hillebrand, T. R., Hoffman, M. J., Huybrechts, P., Jourdain, N. C., Klose, A. K., Langebroek, P. M., Leguy, G. R., Lowry, D. P., Mathiot, P., Montoya, M., Morlighem, M., Nowicki, S., Pattyn, F., Payne, A. J., Quiquet, A., Reese, R., Robinson, A., Saraste, L., Simon, E. G., Sun, S., Twarog, J. P., Trusel, L. D., Urruty, B., Van Breedam, J., van de Wal, R. S. W., Wang, Y., Zhao, C., and Zwinger, T. (2024). Evolution of the antarctic ice sheet over the next three centuries from an ismip6 model ensemble. *Earth's Future*, 12(9):e2024EF004561. e2024EF004561 2024EF004561.

Shepherd, A., Ivins, E., Rignot, E., Smith, B., Van Den Broeke, M., Velicogna, I., Whitehouse, P., Briggs, K., Joughin, I., Krinner, G., et al. (2018). Mass balance of the Antarctic Ice Sheet from 1992 to 2017. *Nature*, 558:219–222.

Shepherd, A., Ivins, E., Rignot, E., Smith, B., Van Den Broeke, M., Velicogna, I., Whitehouse, P., Briggs, K., Joughin, I., Krinner, G., et al. (2019). Mass balance of the Greenland Ice Sheet from 1992 to 2018. *Nature*, 579:233–239.

Shepherd, A., Ivins, E., Rignot, E., Smith, B., van den Broeke, M., Velicogna, I., Whitehouse, P., Briggs, K., Joughin, I., Krinner, G., et al. (2021). Antarctic and greenland ice sheet mass balance 1992–2020 for IPCC AR6 (version 1.0), UK Polar Data Centre, Natural Environment Research Council, UK Research & Innovation [data set].

Shepherd, A., Ivins, E. R., Geruo, A., Barletta, V. R., Bentley, M. J., Bettadpur, S., Briggs, K. H., Bromwich, D. H., Forsberg, R., Galin, N., et al. (2012). A reconciled estimate of ice-sheet mass balance. *Science*, 338(6111):1183–1189.

Smith, R. S., Mathiot, P., Siahaan, A., Lee, V., Cornford, S. L., Gregory, J. M., Payne, A. J., Jenkins, A., Holland, P. R., Ridley, J. K., et al. (2021). Coupling the uk earth system model to dynamic models of the greenland and antarctic ice sheets. *Journal of Advances in Modeling Earth Systems*, 13(10):e2021MS002520.

Stokes, C. R., Abram, N. J., Bentley, M. J., Edwards, T. L., England, M. H., Foppert, A., Jamieson, S. S., Jones, R. S., King, M. A., Lenaerts, J. T., et al. (2022). Response of the east antarctic ice sheet to past and future climate change. *Nature*, 608(7922):275–286.

Vizcaíno, M., Mikolajewicz, U., Jungclaus, J., and Schurgers, G. (2010). Climate modification by future ice sheet changes and consequences for ice sheet mass balance. *Climate Dynamics*, 34(2):301–324.

Wiese, D., Yuan, D., Boening, C., Landerer, F., and Watkins, M. (2022). JPL GRACE and GRACE-FO mascon ocean, ice, and hydrology equivalent water height RL06.1M CRI filtered version 3.0, ver. 3.0 PO.DAAC. Dataset accessed [2023-11-20] at https://doi.org/10.5067/temsc-3mj62, JPL Physical Oceanography Distributed Active Archive Center.

Williams, R. G., Goodwin, P., Ridgwell, A., and Woodworth, P. L. (2012). How warming and steric sea level rise relate to cumulative carbon emissions. *Geophysical Research Letters*, 39(19).

A Appendix Figures and Tables

Table A.1: ADF statistics for Ice Sheets 1993M5 - 2011M1 (T=213)

Variable	Null Hypothesis	Selected lag length	t_{ADF}	Estimated Root	$\hat{\sigma}$	AIC
$\Delta^2 Gr$	I(3)	12	-5.88^{**}	-0.28	2.27	1.75
ΔGr	I(2)	13	-2.41	0.91	2.24	1.73
Gr	I(1)	11	1.52	1.00	2.39	1.85
$\Delta^2 WA$	I(3)	12	-5.36^{**}	-0.13	1.92	1.42
ΔWA	I(2)	13	-3.35	0.89	1.87	1.37
WA	I(1)	12	0.63	1.00	1.91	1.41
$\Delta^2 EA$	I(3)	13	-4.85^{**}	-0.44	2.86	2.22
ΔEA	I(2)	13	-3.37	0.83	2.80	2.17
EA	I(1)	13	-0.47	1.00	2.82	2.19

Note: Estimated with a Constant, Trend, and Seasonals allowing for up to 13 lags.
* denotes rejection of the null at 5% while ** denotes rejection of the null at 1%.

Table A.2: Testing Multivariate Hypotheses of I(1) vs. I(2)

		Gr_t	WA_t	EA_t	t	Model 1 $\chi^2(1)$	Model 2 $\chi^2(2)$
Is the trend-adjusted Greenland Ice Sheet $I(1)$?							
$\mathscr{H}_1$	β_1'	1.0	-	-	*	11.06 [0.001]**	14.41 [0.001]**
Is the trend-adjusted West Antarctic Ice Sheet $I(1)$?							
$\mathscr{H}_2$	β_1'	-	1.0	-	*	8.53 [0.003]**	7.63 [0.021]*
Is the trend-adjusted East Antarctic Ice Sheet $I(1)$?							
$\mathscr{H}_3$	β_1'	-	-	1.0	*	9.34 [0.002]**	9.07 [0.011]*

Note: p-values in brackets. * denotes rejection of the null at 5%
while ** denotes rejection of the null at 1%.

Table A.3: Estimated relationship between Ocean Heat Content and Stochastic Ice loss Trend

	$\Delta StI2$	$\Delta StI2$	$\Delta StI2$
OHC_{0-700}	2.09		
	[2.01]		
$OHC_{700-2000}$		-3.67	
		$[-1.05]$	
$OHC_{2000-6000}$			-13.00
			$[-3.79]$
$trend$	-0.40	-0.18	-0.13
	$[-5.98]$	$[-2.27]$	$[-2.97]$

Note: HAC t-statistics in square brackets

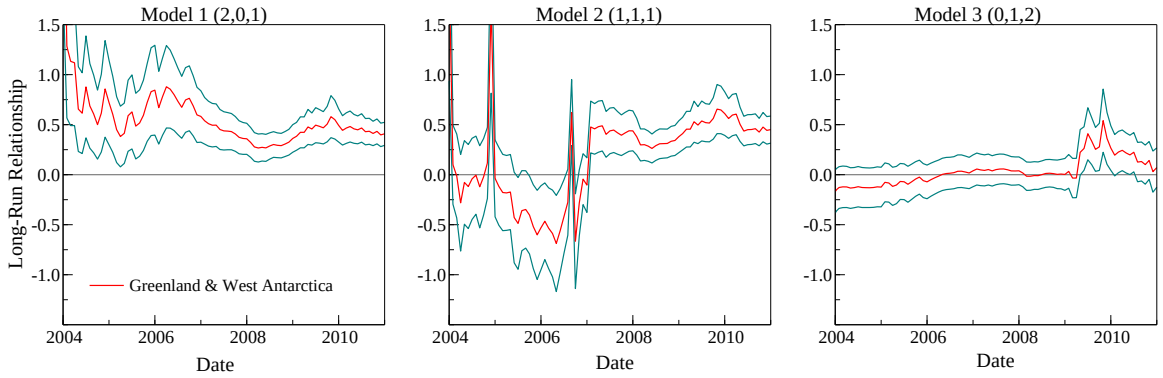

Note: Estimates start in January 1994 and are estimated using an expanding window ending initially in January 2004.

Figure A.1: Recursive Estimates the Long-run relationship between Greenland and Antarctica

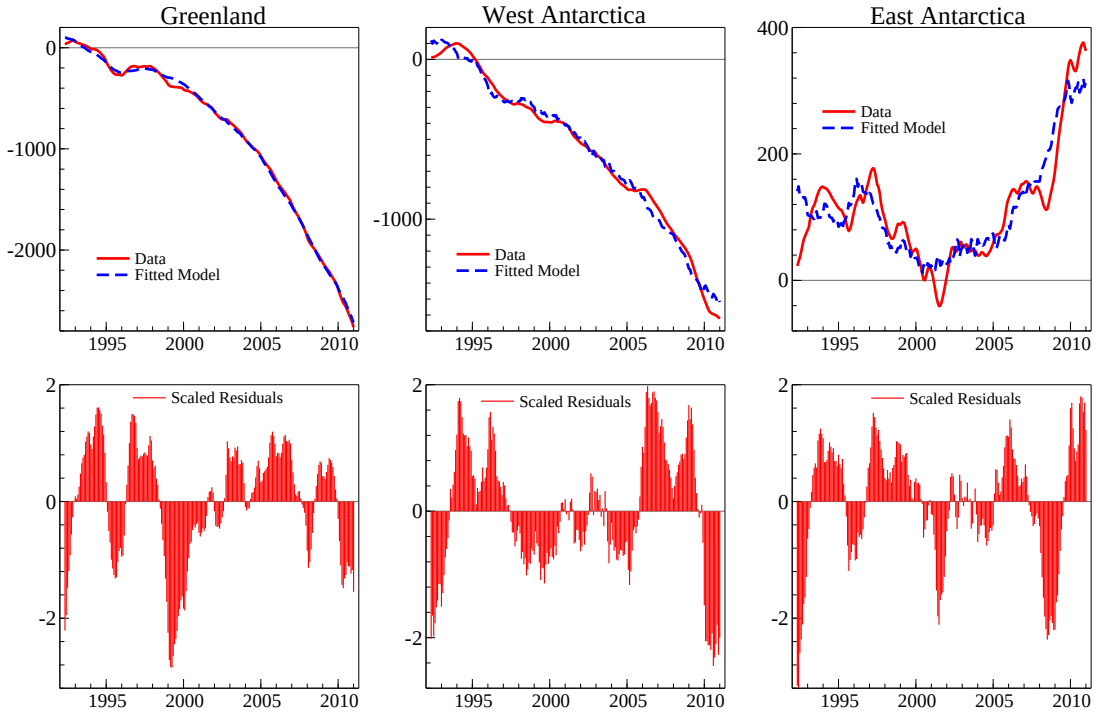

Figure A.2: Estimated Models of Stochastic and Linear Trends (in Gt, May 1992 - Jan 2011)

Table A.4: Forecast Performance Relative to a AR(12) Model (Feb. 2011 - Dec. 2020) evaluated using IMBIE mass anomalies from Otosaka et al. (2023)

	Greenland			**West Ant.**			**East Ant.**			**Joint**$^{\alpha}$		
	R	**Ur**	**Sr**	**R**	**Ur**	**Sr**	**R**	**Ur**	**Sr**	**R**	**Ur**	**Sr**
AR	1.00	1.00	0.27	1.00	1.00	**0.18**	1.00	1.00	1.09	1.00	1.00	**0.58**
M0	0.83	0.83	0.32	5.75	5.75	0.90	0.66	0.66	**0.37**	1.33	1.33	0.62
M1	**0.43**	0.45	0.14	**0.54**	0.64	0.55	1.44	1.33	1.23	0.90	0.90	0.86
M2	0.60	0.60	**0.12**	1.16	1.16	0.30	2.17	2.17	6.14	1.07	1.07	1.17
M3	0.82	**0.36**	0.19	0.61	**0.54**	0.60	**0.09**	**0.61**	1.17	**0.78**	**0.72**	0.74

Note: Performance is calculated as the square root of the average squared error from a single path of forecasts across all horizons and relative to the baseline model. Bolded values indicate best performance.
Models: AR: Baseline AR(12); M0: restricted VAR; M1 Model 1; M2 Model 2; M3 Model 3.
R: Long-run over-identifying restrictions imposed. Ur: No Long-run over-identifying restrictions imposed.
Sr: Smooth Robust Transformation with $w_1 = 1$ and $w_2 = w_3 = 36$.
$^{\alpha}$Calculated as the determinant of the system of ice sheets following Clements and Hendry (1993).

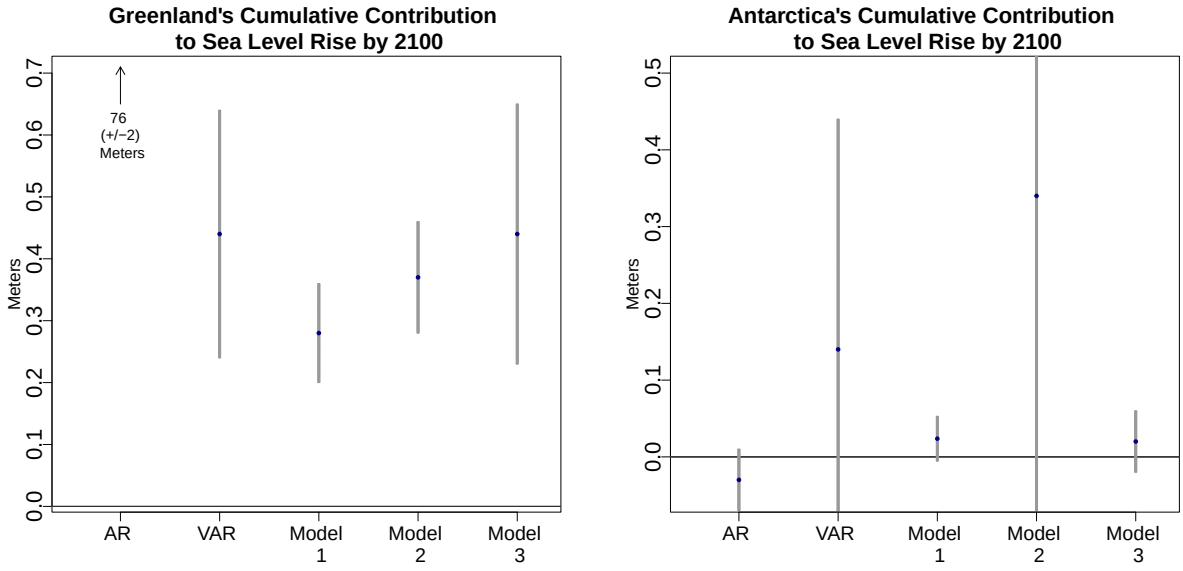

Note: Calculated as the forecast of ice sheet mass anomalies at the beginning of 2100 relative to the average 1992-1998 divided by 360,000 to account for ocean surface area and to convert from Gigatonnes into meters of global mean sea-level rise. The grey bars represent the +/- 1 s.d. forecast and parameter estimation uncertainty for the model forecasts.

Figure A.3: Alternate Projections of Ice Sheet Contributions to GMSLE rise by 2100